



Atlin TGI, Part II: Regional Geology and Mineralization of the Nakina Area (NTS 104N/2W and 3)

By Mitchell G. Mihalynuk¹, Stephen T. Johnston², Joseph M. English², Fabrice Cordey³,
Michael E. Villeneuve⁴, Lin Rui⁵ and Michael J. Orchard⁶

KEYWORDS: *Geology, mineralization, volcanogenic massive sulphide, exhalite, sepiolite, talc, geochronology, fusulinacean, radiolarian, fossil, aeromagnetic survey, Cache Creek terrane, Nahlin fault, Nakina, Atlin.*

INTRODUCTION

We report on the second and final year of geological mapping in the Nakina area, conducted under the Atlin Targeted Geoscience Initiative (TGI). Principal aims of the TGI are to create a legacy of high quality geoscience data that will stimulate geological resource exploration, and regional economic development (*see* Atlin TGI - Part I). Geological maps produced as part of the project portray base-line data required for informed land-use decisions or other studies where bedrock geology is a consideration.

Since 1898, when Fritz Miller and his partner Kenneth McLaren discovered rich placers on Pine Creek (Bilsland, 1952), the economic well-being of the Atlin region has been largely tied to the price of gold. Yet, good potential for economic diversification in the mining sector exists because the Atlin area contains a diversity of prospective geological environments. Results of geological mapping in the Nakina area in 2001 (Mihalynuk *et al.*, 2002) affirmed such potential. Results included the discovery of submarine felsic volcanic rocks and extensive hydrothermal deposits of exhalative magnetite; deposits that are common in mining camps where copper, lead and zinc are produced from volcanogenic massive sulphide accumulations. A key host rock in many of these camps is submarine dacite or rhyolite. Felsic volcanic rocks, and the sediments derived from them, have long been considered uncharacteristic of the Cache Creek rocks in the Atlin area. Our mapping showed that clastic strata derived from felsic volcanic rocks are relatively common. Further evidence for prospectivity of Cache Creek rocks comes from discoveries during 2002. Mineralization includes massive sulphide lenses in submarine mafic volcanic rocks at the new Joss'alun discovery (*see* Atlin TGI -Part III), massive pyrrhotite that is probably related to Eocene skarn, a broad zone of quartz-sericite schist in a side canyon of the Nakina River, and industrial mineral occurrences of sepiolite near Mount O'Keefe and talc near Chikoida Mountain.

Results of geological studies presented arise from collaborative partnerships between the BC Ministry of Energy and Mines, Geological Survey of Canada, University of

Victoria, Université Claude Bernard, Simon Fraser University, and the Yukon Government.

LOCATION, ACCESS AND PHYSIOGRAPHY

In 2001, Regional geologic mapping at 1:50 000 scale was conducted across the southeast corner of the Atlin mapsheet, covering the Nakina Lake area and about 70% of the Nakina River area (Figure 1); NTS mapsheets 104N/1 and 2, respectively. Fieldwork in 2002 was originally planned to complete mapping of NTS mapsheet 104N/2 as well as the Sloko River mapsheet, 104N/3. Reduced financial support for field programs in 2002 hampered mapping progress, resulting in incomplete mapping over about 25% of the 104N/3 sheet. Mapsheet 104N/1, 2 and 3 together cover an area of approximately 2400 km² (28 km from north to south and 84 km east to west) that spans a region between 38 and 115 kilometres southeast of the town site of Atlin (Figure 1). It is herein referred to as the "Nakina transect".

Access to the Nakina transect is most effectively achieved using a helicopter charter based out of Atlin. Parts of the transect can also be accessed from lakes large enough for floatplanes. There are no all-season roads within the area. One rough, fire abatement road extends to Kuthai Lake at the northern limit of 104N/3; about a 2.5-hour drive from Atlin. It is suitable for four wheel drive or all-terrain vehicles and requires fording the O'Donnel River and Dixie Lake outflow.

Travel by foot is relatively easy within the Nakina transect. Two heritage footpaths cross the area: the Telegraph and Taku trails. Telegraph Trail was cut diagonally across 104N2 and 3 between 1900 and 1902 as part of an ill-fated telecommunication syndicate (Bilsland, 1952). Most of the durable telegraph wire has been scavenged and put to good use, and much of the route is still well maintained by guide-outfitters. Other parts are overgrown and

¹BC Ministry of Energy and Mines

²University of Victoria

³Université Claude Bernard, Lyon France

⁴Geological Survey of Canada, Ottawa

⁵Paleontological Consultant, Calgary

⁶Geological Survey of Canada, Vancouver

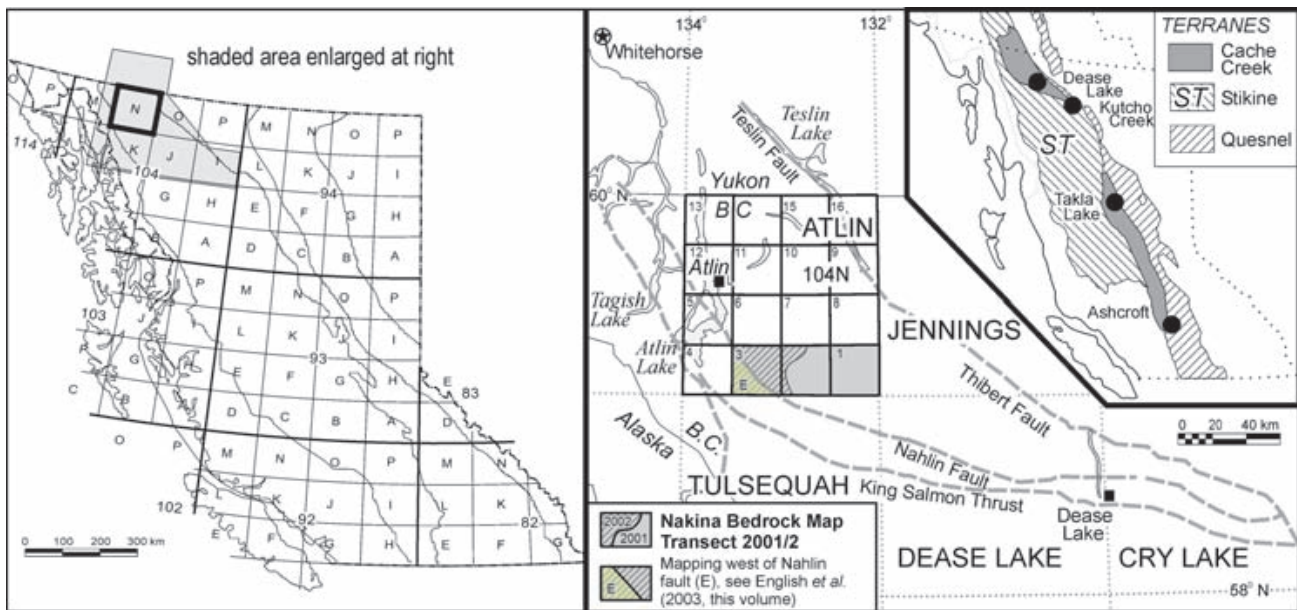


Figure 1. Location of the Atlin Targeted Geoscience Initiative (TGI) Project in northwestern British Columbia. Bold outlined box (104N) shows extent of Atlin TGI aeromagnetic survey. Regional geological mapping surveys were conducted over the eastern and central Nakina transect (104N/1, 2) in 2001 and extended into 104N/3 in 2002.

recognizable only by weathered blazes and beleaguered relicts (Photo 1).

Atlin was linked with tidewater on Taku Inlet by the Taku Trail, which followed the Silver Salmon River in the Nakina area (Figure 2). Except where the route coincides with game trails, it has overgrown with the ebb of foot traffic in the post gold rush era. Off trail, foot passage is easy on dry or well-drained south-facing slopes, which generally have open forest floors between fir, spruce, aspen and pine; or in recent forest fire scars that have yet to establish willow, alder and dwarf birch growth. Foot travel is more challenging on slopes that are north facing and poorly drained, especially near treeline where they can be a tangle of stunted fir and spruce. Canyons along the lower Nakina River and its major tributaries are negotiated with diffi-



Photo 1. Reminders of a bygone era, horseshoes hang along the overgrown Telegraph Trail.

culty; parts are impassable without technical climbing equipment. However, travel along canyons rims is a spectacular treat and many parts are lined with well-trodden goat trails. These canyons are part of the elevated Taku Plateau in the western Nakina transect area; they drain to the Pacific. Topography subsides eastward to the low, swampy Kawdy Plateau (Photo 2), which mainly drains to the Arctic. Most of the Nakina transect area is below tree line, which is around 1400 metres elevation. Mountains are less than 1900 metres elevation, and are relatively easily negotiated on foot. One exception is Paradise Peak at 2100m, which lies just beyond the western boundary of the Nakina transect.

PREVIOUS WORK

Previous regional map coverage of the Nakina transect is of early to mid 1950s vintage (Aitken, 1959), pre-dating the advent of plate tectonics. Thematic revision mapping in the mid to late 1960's by Monger (1975) covered much of



Photo 2. View over the eastern two thirds of the Nakina transect area, from Focus Mountain in east-central 104N/3.

the carbonate-dominated rocks in the central transect area. Monger (1975) pieced together a biostratigraphy and used igneous geochemistry, map relationships, and the recognition of a disrupted ophiolitic succession to show that the Atlin area is composed largely of relict ocean basin crust and oceanic islands. Terry (1977) confirmed this assertion and suggested an analogue in the Pindos ophiolites of Greece. Ash (1994) drew similar conclusions from the ophiolitic ultramafic rocks near the town site of Atlin.

In 1996, a compilation of Atlin geology was completed as part of a provincial mineral potential evaluation (Mihalynuk *et al.*, 1996) available for viewing or download at www.em.gov.bc.ca/Mining/Geolsurv/MapPlace. Sources of information drawn upon for the compilation included mineral tenure assessment reports, 1:50 000-scale revision mapping (Bloodgood and Bellefontaine, 1990; Lefebure and Gunning, 1988; Mihalynuk and Smith, 1992) and 1978 Regional Geochemical Survey (RGS) results (BCMCM, 1978). Archival stream sediment samples were reanalysed for a broad range of elements, including gold, and published in 2000 (Jackaman, 2000; available for download at www.em.gov.bc.ca/Mining/Geolsurv/rgs/sheets/104n.htm). In the same year, a regional aeromagnetic survey of the entire Atlin map sheet, about 14 000 square kilometres was conducted (*e.g.* Dumont *et al.*, 2001a, b, c; Lowe and Anderson, 2002) as the first phase of the Atlin TGI. Evaluation of the aeromagnetic data is ongoing with future publication anticipated, together with publication of results from other branches of the TGI project (*see* TGI Part I).

REGIONAL GEOLOGY

Rocks of the Nakina transect area can be broadly separated into one of four distinct packages. From oldest to youngest (and most to least abundant), they are: Mississippian to Early Jurassic Cache Creek oceanic rocks; Early to Middle Jurassic Laberge wacke and shale; Middle Jurassic,

post-tectonic intrusions; and Early Eocene continental arc volcanic, comagmatic plutonic, and sedimentary rocks of the Sloko Group.

Most of the eastern transect area is underlain by Cache Creek oceanic crustal and supracrustal strata and Middle Jurassic bodies that intrude them. They are separated by the crustal-scale Nahlin fault from strata the Laberge Group an overlying Sloko Group in southwest 104N/3. Sloko basalt may also occur east of the Nahlin fault in the Pike Lake area. All rocks older than the ~172Ma Jurassic plutons have been folded and faulted; most recently by southwest-verging folds and thrusts, between 174 and 172 Ma.

Geological observations reported here are new or updated in 2002, mainly for mapsheets 104N/2 and 3. For information on the geology of 104N/1, including an overview on nomenclature for Cache Creek rocks, refer to (Mihalynuk *et al.*, 2002) and sources therein.

CACHE CREEK ROCKS

As early as 1953, M.L Thompson recognized the Tethyan affinity of fusulinid faunas collected from Cache Creek rocks in the Atlin area (*in* Harker, 1953); clearly exotic with respect to the adjacent non-Tethyan rock packages. This demonstrably exotic aspect of the Atlin rocks was pivotal to the development of the “Terrane Hypothesis” (Coney *et al.*, 1980). Cache Creek rocks continue to play a leading role in our understanding of the Canadian Cordillera, and perhaps the best exposures are in the Nakina transect.

Within the transect, Cache Creek rocks comprise four domains (Figure 2): eastern and western domains are dominated by basalt, chert and ultramafite (Disella and Goldbottom domains); a central domain is dominated by carbonate and lesser chert (Sinwa domain); and a northern heterolithic domains are comprised of well bedded, folded and faulted chert (Chikoida domain), and carbonate and volcanic rocks (Blackcaps domain). Most of the eastern

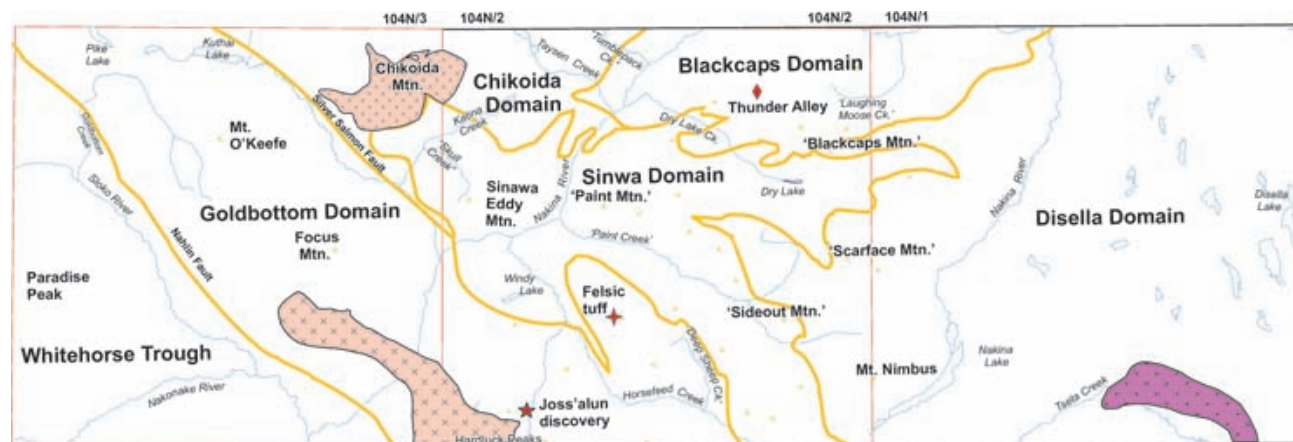


Figure 2. Geologic domains of the Nakina transect area in relation to key geographic and geological features.

domain lies within 104N/1 and is described by Mihalynuk *et al.* (2002).

Regional metamorphic grade of the Northern Cache Creek terrane is prehnite-pumpellyite facies, although thermal upgrading to biotite and, rarely, garnet-grade is observed around large plutons. Local blueschist grade metamorphism is known from the Dease Lake area (Monger, 1969), but is not known in the Nakina transect. Sparse conodont alteration indices (CAI) from Cache Creek rocks in the Nakina area are generally slightly higher than the metamorphic grade as indicated from authigenic mineralogy (*see English et al.*, 2003, this volume).

We address new observations in a stratigraphic context, from lowest (mantle) to highest (platformal carbonate) as they would appear in an undisturbed, idealized oceanic crustal section.

MANTLE: SERPENTINIZED HARZBURGITE

Harzburgite is an ultramafic rock composed mainly of olivine and orthopyroxene with accessory clinopyroxene and chromite. Orthopyroxene and chromite grains commonly form streaky clusters outlining a high temperature fabric interpreted as having a mantle origin (Photo 3a). This fabric is cut by undeformed pyroxenite dikelets (Photo 3b), also of presumed mantle origin. Harzburgite is the domi-



Photo 3. (a) mantle tectonite fabric outlined by serpentinitized relicts of sheared orthopyroxene. (b) undeformed pyroxenite dikelet cuts mantle fabrics.

nant protolith within the Nahlin ultramafic body and forms a coherent 1.5 x 15 km, dun-weathering body, best exposed south of the Nakina River in 104N/2W (Figures 2, 3). At that locality, it is bound to the west by gabbro, which passes upwards into submarine basalt, host to massive sulphide mineralization at the Joss'alun occurrence (*see Mihalynuk et al.*, 2002b, this volume). To the east are fault panels of wacke and mafic volcanoclastics with lesser serpentinite lenses interpreted as part of an accretionary prism. North of the Nakina River, the harzburgite body is structurally interleaved with panels of bright green serpentinite. Bright orange quartz-carbonate (listwanite) alteration of serpentinite occurs where it has been extensively veined, commonly near faults (*see structural styles following*). Within the main harzburgite body, there is no deformational fabric that post-dates emplacement of pyroxenite dikelets, indicating that strain was highly partitioned, or that the harzburgite acted as a rigid body during emplacement.

SERPENTINITE MÉLANGE

Much of the low-lying area between the Sloko and Silver Salmon rivers is underlain by serpentinite mélangé (Figure 3). Knockers up to several square kilometres in area vary in a relatively consistent manner from west to east. A western belt contains mainly of harzburgite and gabbro knockers; followed by diorite and basalt knockers, then chert with minor basalt, and finally, basalt with minor chert. In both the eastern and western-most belts, serpentinite may comprise more than 50% of areas several square kilometres in size. In the intervening belts, serpentinite is estimated to comprise less than 10% of the rock volume.

Near with the easternmost limit of the serpentinite-rich mélangé belts are panels of thinly bedded siltstone. Immediately west, mint green volcanoclastic rocks abruptly increase in abundance, comprising blocks up to mountain-size. Sparse exposures in valleys between the blocks are comprised of scaly serpentine. Swampland west of the Silver Salmon River in central 104N/3E is underlain mainly by serpentinite. Knockers, some more than 400 metres across, stick up out of the swamps. They are resistant buttress to rat-tails of serpentinite that point in the direction of ice flow during the last continental glaciation; lakes occupy the scoured up-ice side of the knockers (*see Lowe et al.*, 2003).

Chert is subordinate to mafic volcanics, but it also comprises blocks the size of entire mountainsides. Focus Mountain is part of one such block, which is composite of many fault-bounded panels that are intermittently exposed over an area of 3.5 km by 10 km. Serpentinite occurs along the boundaries of the Focus Mountain domain as it does along all major blocks. Serpentine becomes increasingly dominant towards the west, so that the mélangé belt near the Nahlin Fault is composed mainly of serpentinite, and knockers generally less than 1 or 2 km in maximum dimension. An exception is the harzburgite at Hardluck Peaks, south of the Nakina River, which forms a semi-coherent, 1.5 km-wide body that parallels the structural grain for ~15 km. North of the Nakina River, the harzburgite body is structurally disaggregated, and comprises the dominant

knocker type within the western part of the mélangé belt. Gabbro, and hornblende diorite are subordinate to the harzburgite, increasing in abundance to the east. The large size of some knockers argues against entrainment of knockers as “xenoliths” during serpentine diapirism or subduction zone backflow, at least when compared to modern analogues. Rather, tectonic juxtaposition within a subducting margin setting probably occurred by two processes: first, by exhumation of the mantle (but not necessarily to the level of subaerial/subaqueous exposure) during initiation of subduction; and later, by offscraping of oceanic sediment and crustal protruberances such as ocean islands from the subducting slab.

GOLDBOTTOM CREEK GABBRO

Gabbro crops out over several square kilometres at the headwaters of Goldbottom Creek, south of Mount O’Keefe. It is a folded, sheet-like body that displays an intrusive contact with overlying mafic volcanic rocks and fault contact with underlying ultramafic, mafic and quartz-rich clastic rocks. It is interpreted as an allochthonous sheet. Chert in the footwall of the allochthon is carried on a southwest-verging thrust that has been deformed by open folds; similar to in style to those that control the map pattern distribution of the allochthon. Gabbro within the allochthon appears to have been attenuated by dilatant, high-angle faults that are invaded by serpentinite. Dilatant faults are probably kinematically linked to motion on the Nahlin Fault (*see* Nahlin fault).

SHEETED DIKE COMPLEX?

Nowhere in the northern Cache Creek terrane has an intact-sheeted dike complex been found. However, crowded sets of mafic dikes occur within the gabbro-basalt succession southwest of Mount O’Keefe. Knockers composed of multiple dikes may also be relicts of a sheeted dike complex, but they are generally less than 10m across; too small to permit confirmation.

MAFIC PLUTONS AND PLAGIOGRANITE

Hornblende diorite or tonalite, representatives of the intrusive magmatic parts of the crustal section, are also found as knockers together with relicts of harzburgite within serpentinite mélangé. Below tree line near Tseta Creek (104N/1), a >1 km² area of diorite is intruded by an irregular network of pegmatitic plagiogranite dikes. These rocks may be part of an intact oceanic crustal section. Plagiogranite dikes are generally less than 0.5 m thick. They are composed mainly of plagioclase and hornblende with about 10% interstitial quartz and accessory titanite and zircon. They are undeformed and weakly metamorphosed. Plagioclase is partly altered to prehnite and, possibly, the zeolite phillipsite (Photo 4a). Hornblende is nearly pristine, with only the slightest traces of chlorite alteration (Photo 4b).

BASALTIC VOLCANICLASTICS ‘BLACKCAPS’ ASSEMBLAGE

Basaltic volcaniclastic rocks are the dominant Cache Creek unit within the Nakina transect. Monger (1975) included such rocks within the Nakina Formation. English *et al.* (2002) recognized geochemically distinct volcanic units that probably formed in different tectonic environments. The most abundant mafic volcaniclastic unit they called the ‘Blackcaps’ assemblage, we use their terminology here (Figure 3).

‘Blackcaps’ assemblage basaltic volcaniclastics commonly display well-preserved, aphanitic lapilli and ash-sized fragments despite widespread replacement by prehnite, pumpellyite, calcite and chlorite. Colour of fresh surfaces is distinctive: mint green with a grey or pinkish cast caused by filaments (fine shear bands) of clay and iron oxides. Weathered outcrop surfaces are orange, dark brown or olive green. Gabbro and rare plagiogranite intrude the basalt (*see* above). Near ‘Blackcaps Mountain’, volcaniclastics are interbedded with Middle Triassic chert (Table 1). Disrupted chert beds or olistostromal layers, with

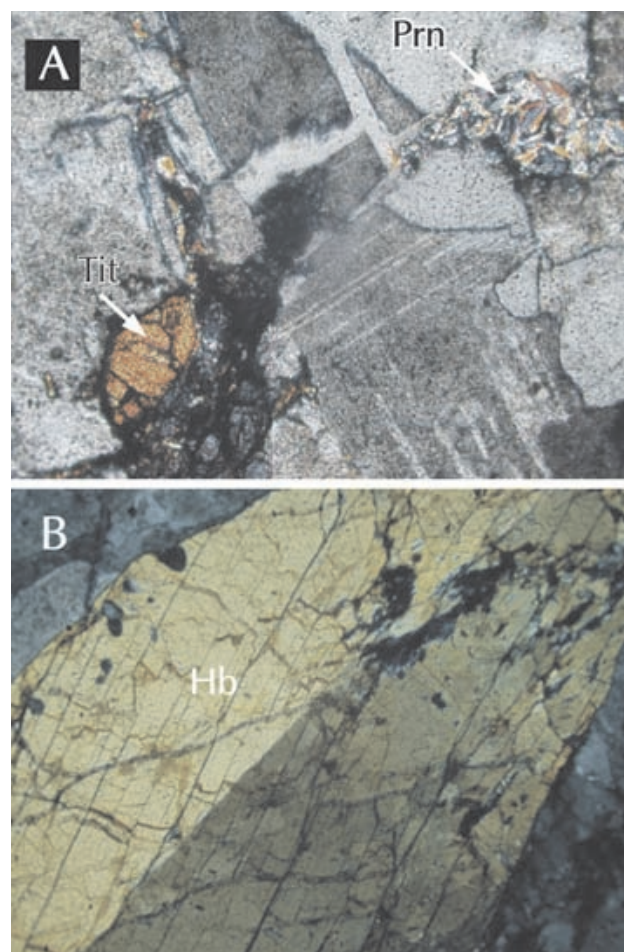


Photo 4. (a) Photomicrograph of plagiogranite. Quartz and feldspar dominate the section, accessory titanite (Tit) and authigenic prehnite (Prn) are labelled. (b) Basal section of hornblende (Hb) shows only the slightest traces of chlorite alteration, most hornblende in the sample is less altered.

Nakina transect

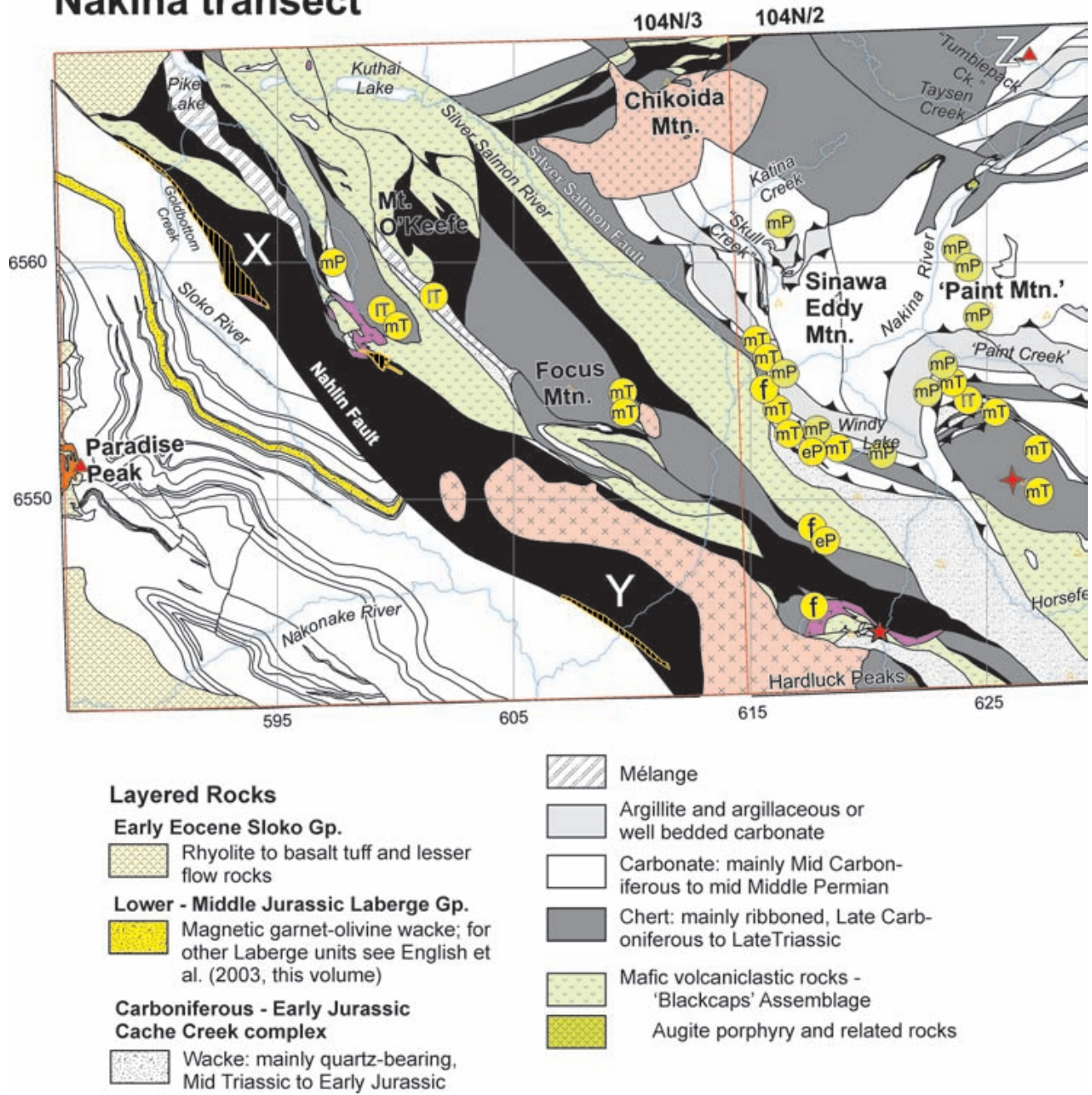


Figure 3. Simplified geology map of the Nakina transect.

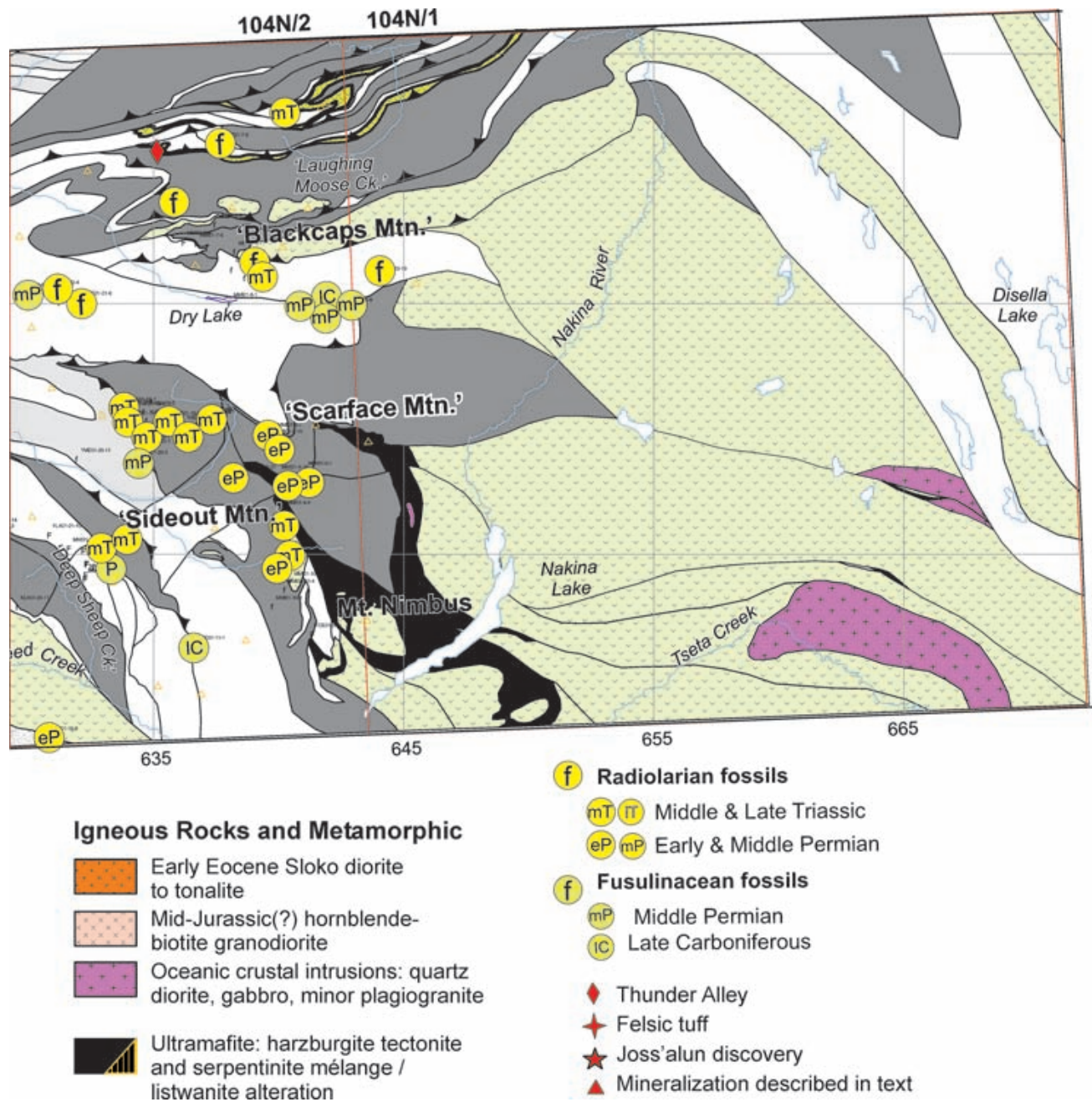


Figure 3. continued

chert blocks up to the size of locomotives, are more common than conformable beds. Carbonate blocks are rare by comparison. Homogeneous tuff can comprise entire mountainsides such as south of eastern Kuthai Lake.

Geochemical analyses of basaltic volcanoclastic rocks have shown them to be mainly of island arc thoeiite composition, according to (English *et al.*, 2002). These authors propose a primitive arc setting, possibly part of the Kutcho-Sitlika arc system (*see also* (Mihalynuk and Cordey, 1997; Schiarizza *et al.*, 1998; Childe and Thompson, 1998).

CHERT SUCCESSIONS

Chert and other siliceous sediment are the dominant rock types within the northern Cache Creek terrane. In the Atlin and Teslin areas, little was known about these rocks, including their age, prior to the work of Cordey (*e.g.* Cordey *et al.*, 1991). Radiolarian age data did not exist for the Nakina transect area prior to initiation of the Atlin TGI mapping program in 2001. Currently, 92 samples have been processed for radiolaria (Table 1), with the results of an additional 19 pending. This data permits an unprecedented level of understanding of stratigraphy and structure within pelagic, hemipelagic, and interbedded rocks of the Nakina transect.

Four types of chert are common within the Nakina transect. These are divisible on the basis of lithology and, apparently, age (Table 1). Type 1 occurs as thick accumulations of medium to light grey or grey green, irregularly ribboned, recrystallized and indurated chert of probable Late Paleozoic age (Photo 5). In glacially polished outcrops it can form unbroken surfaces metres across. Chert beds are typically 2-6 cm thick with 2 to 5 mm, orange, tan or green-weathering, dark grey argillaceous partings. Intercalations of other lithologies are rare. Type 1 chert underlies most of the northern flank of the 'Blackcaps' domain between the Nakina River and tree line. It is well exposed above the confluence of Taysen Creek. It also underlies a large part of the Katina Creek valley south of the Chikoida Mountain stock (Figures 2 and 3).

Type 2 chert is relatively uncommon. It is planar bedded and intercalated with clastic limestone of probable Permian age. It occurs between Type 1 chert and accumulations of carbonate, and is best developed in the Blackcaps domain.

Type 3 is planar ribboned, mainly black, grey and tan chert that is generally not strongly recrystallized. Intercalations of other lithologies, particularly mafic volcanoclastic strata, are common. Outcrops are rubbly-weathering and pieces of chert beds can be easily plucked from the outcrop. This type of chert is widespread; it can comprise sections hundreds of metres thick. For example, chert underlying Focus Mountain is largely composed of this type. Microfossils extracted are typically of Middle Triassic age.

Type 4a is massive, featureless argillaceous chert in layers more than 5 metres thick. These display joint planes that extend the width of the unit (in contrast to type 3), giving it the appearance of a homogeneous, dark intrusive or



Photo 5. Irregular bedding in ribbon chert seems to be a characteristic of Paleozoic chert in the Nakina transect.

volcanic unit from a distance. Type 4b chert is ribboned and disrupted or grades into argillaceous chert. It may be interbedded with wacke containing a large proportion of volcanic quartz grains. It includes broken formation, which is generally restricted aurally to bands less than 100m thick; too narrow to be mapped to scale on Figure 3. Radiolaria obtained from Type 4 chert are most commonly of Middle to Late Triassic age. In broken formation, a mixture of ages can be expected.

Many of the chert successions within the transect are lithologically variable and range widely in age. No subdivision is attempted in such places. Indeed, it is possible that further micropaleontological age dating may show that most, if not all, thick successions range broadly in age. Because of the slow rate of biogenic silica accumulation, a broad range of ages is to be expected in thick chert successions. In practice, however, this appears not always to be the case. For example, the densest radiolarian age data coverage is of chert coring an anticline in central 104N/2E. Microfossils were collected from 18 sites more-or-less evenly distributed for 3.5 km across strike and 3 km along strike (Figure 4). Where diagnostic faunas were recovered, they are of Middle Triassic age (Table 1, *see also*: Structural Styles). Structurally overlying carbonate contains Permian fusulinaceans (Figure 4, Table 2) and conodonts (*i.e.* YME01-20-4, Table 3).

Despite an explosion of radiolarian age data attributable to the Atlin TGI, our understanding of Cache Creek chert successions is still rudimentary. Future work should critically evaluate the four-unit subdivision presented here.

LIMESTONE-CHERT BRECCIA

A great structural thickness of Type 1 chert and overlying units are intermittently exposed below treeline in the northern Blackcaps domain. An irregular limestone unit, possibly comprised of olistostromal blocks up to 100m long and 40m thick, overlies the chert. Next is a layer of chert-argillite-limestone breccia, 5 to more than 30 m thick. Clasts of limestone are mainly angular to subround, of peb-

TABLE 1
RADIOLARIAN FOSSIL IDENTIFICATIONS BY F. CORDEY

Station Number	NAD 83 UTM E	Zn8 UTM N	Lithology	Preservation	Radiolarian taxa Observations	Age
FCO01-17-05-1	627465	6552526	black siliceous argillite	poor	<i>Triassocampe</i> sp., indeterminate <i>Oertlispongidae</i> , abundant sponge spicules	Middle Triassic
FCO01-17-08	627454	6552091	black siliceous argillite	poor	<i>Saitoum</i> sp., <i>Triassocampe</i> sp., indeterminate <i>Oertlispongidae</i> , sponge spicules, black clays	Middle Triassic
FCO01-17-09a	627300	6551162	black ribbon chert	moderate	<i>Pseudostylosphaera</i> sp., <i>Tritortis</i> sp., <i>Triassocampe</i> sp., indeterminate <i>Oertlispongidae</i> , rare sponge spicules	Middle Triassic
FCO01-17-09b	627300	6551162	black ribbon chert	poor	<i>Triassocampe</i> sp., indeterminate <i>Oertlispongidae</i> , sponge spicules	probably Middle Triassic
FCO01-17-10	627525	6550753	grey ribbon chert	poor to moderate	<i>Plafkerium</i> sp., <i>Pseudostylosphaera compacta</i> , <i>Yeharaia</i> sp.	Middle Triassic
FCO01-17-12	627963	6550672	grey ribbon chert	poor	<i>Plafkerium</i> sp., <i>Pseudostylosphaera</i> sp., <i>Yeharaia</i> sp.	Middle Triassic
FCO01-17-13a	640014	6550775	grey ribbon chert	poor to moderate	<i>Plafkerium</i> sp., <i>Triassocampe</i> sp.	Triassic
FCO01-17-13b	640014	6550775	grey ribbon chert	poor to moderate	<i>Plafkerium</i> sp., <i>Tritortis</i> sp., <i>Yeharaia</i> sp., <i>Oertlispongids</i>	Middle Triassic
FCO01-17-14	628197	6551020	grey ribbon chert	moderate	<i>Pseudostylosphaera</i> sp., "narrow" <i>Triassocampe</i> sp.	Middle Triassic
FCO01-18-02	637043	6555432	black siliceous argillite	poor	"narrow" <i>Triassocampe</i> sp., sponge spicules, indeterminate spumellarians	Middle Triassic
FCO01-18-03	636903	6555390	grey ribbon chert	poor	<i>Triassocampe</i> sp., indeterminate spumellarians	Triassic
FCO01-18-04	636854	6555307	black siliceous argillite	poor	<i>Pseudostylosphaera compacta</i> , <i>Triassocampe</i> sp.	Middle Triassic
FCO01-18-05	636750	6555238	green siliceous argillite interbed.w. grey ribbon chert	poor	"narrow" <i>Triassocampe</i> sp.	Middle Triassic
FCO01-18-06	636562	6555160	black ribbon chert	poor	? <i>Tritortis</i> sp., indeterminate spumellarians, "narrow" <i>Triassocampe</i> sp., rare sponge spicules.	Middle Triassic
FCO01-18-07	636176	6555122	grey ribbon chert	very poor	recrystallized spumellarians, sponge spicules	indeterminate
FCO01-18-09	633650	6555270	dark grey ribbon chert	poor	<i>Pseudostylosphaera</i> sp., <i>Triassocampe</i> sp., <i>Yeharaia</i> sp.	Middle Triassic
FCO01-18-11	634746	6554724	dark grey ribbon chert	poor to moderate	abundant spumellarians, <i>Pseudostylosphaera</i> sp., "narrow" <i>Triassocampe</i>	Middle Triassic
FCO01-19-01	634429	6554348	black ribbon chert	poor	fragments of recrystallized spumellarians and nassellarians including <i>Triassocampe</i> or <i>Yeharaia</i>	Triassic
FCO01-19-03	634467	6554762	black chert interbed. w. green brown argillite	poor	rare spumellarians, mostly sphaeromorphs and indeterminate morphotypes	indeterminate
FCO01-19-04	634723	6555343	black siliceous argillite	poor	fragments of twisted spines, rare sphaeromorphs, rare sponge spicules	probably Triassic
FCO01-19-05	634615	6555708	grey siliceous argillite	poor	fragments of twisted spines, rare nassellarians, sponge spicules	probably Triassic
FCO01-19-06	634249	6555660	grey ribbon chert	moderate	? <i>Pararuesticyrtium</i> sp., ? <i>Paurinella</i> sp., <i>Pseudostylosphaera</i> sp., <i>Triassocampe</i> sp., <i>Tritortis</i> sp., abundant large spumellarians	Middle Triassic
FCO01-19-07	633870	6555845	grey ribbon chert	moderate	<i>Pseudostylosphaera compacta</i> , <i>Triassocampe</i> sp.	Middle Triassic
FCO01-19-08	633727	6555772	grey ribbon chert	poor	rare nassellarians	Mesozoic
FCO01-19-14	633974	6555303	grey ribbon chert	moderate	<i>Pseudostylosphaera compacta</i> , <i>Triassocampe</i> sp.	Middle Triassic
FCO01-20-01	634454	6554191	black ribbon chert	good	<i>Paurinella</i> sp. cf. <i>aequispinosa</i> , <i>Plafkerium</i> sp., <i>Poulpus</i> sp., <i>Pseudostylosphaera compacta</i> , <i>Triassocampe</i> sp., sponge spicules	Middle Triassic
FCO01-20-11	631940	6553815	black ribbon chert	moderate	<i>Eptingium</i> sp., <i>Oertlispongus</i> sp., <i>Paurinella aequispinosa</i> , <i>Plafkerium</i> sp., <i>Pseudostylosphaera compacta</i> , <i>Triassocampe</i> sp.	Middle Triassic
FCO01-21-06	632100	6560081	siliceous argillite (with clasts and blocks)	poor	sponge spicules, spumellarians, no structures	indeterminate
FCO01-21-08	632897	6560056	black siliceous argillite	very poor	sponge spicules, recrystallized spumellarians, no structures	indeterminate
FCO01-23-03b	630968	6560595	silicified limestone (stratigraphic contact between pillows and limestone)		silica fragments	indeterminate

Table 1, continued

Station Number	NAD 83 UTM E	Zn8 UTM N	Lithology	Preservation	Radiolarian taxa Observations	Age
FCO01-23-04	630789	6560519	grey ribbon chert (from isolated outcrop in fault zone)	poor to moderate	<i>Pseudostylosphaera</i> sp., <i>Triassocampe</i> sp., <i>Yeharaia</i> sp., fragments of <i>Oertlispongidae</i>	Middle Triassic
FCO01-28-06	618074	6650601	fine-grained tuffaceous argillite (protochert)	very poor	rare sphaeromorphs and sponge spicules, matrix fragments	indeterminate
FCO01-28-13	620270	6551311	grey ribbon chert	good	<i>Pseudostylosphaera</i> sp., <i>Triassocampe</i> sp., <i>Yeharaia</i> sp., <i>Tritortis</i> sp.	Middle Triassic
FCO01-29-02	618008	6551852	dark grey ribbon chert	moderate	<i>Entactinia</i> sp., <i>Haploaxon</i> sp., <i>Latentifistula</i> sp., <i>Pseudoalibaillella scalprata</i>	Early Permian
FCO01-29-10	615601	6552589	green volcanic siltstone	very poor	sphaeromorphs and sponge spicules, matrix fragments	indeterminate
FCO01-29-14	616051	6553416	black ribbon chert	moderate	<i>Plafkerium</i> sp., <i>Pseudostylosphaera compacta</i> , <i>Yeharaia</i> sp., <i>Triassocampe</i> sp.	Middle Triassic
FCO01-29-15	616219	6553627	black ribbon chert	poor	<i>Entactinia</i> sp., Latentifistulidae fragments, recrystallized spumellarians	Late Paleozoic
FCO02-01a	609852	6553938	grey chert, broken fm	moderate	Oertlispongids, <i>Pseudostylosphaera</i> sp., <i>Triassocampe</i> sp., <i>Yeharaia</i> sp.	Middle Triassic
FCO02-01b	609852	6553938	grey chert, broken fm	good	<i>Pseudostylosphaera japonica</i> , <i>Triassocampe</i> sp., <i>Yeharaia</i> sp.	Middle Triassic; late Anisian-Ladinian
FCO02-02	587872	6566122	tuffaceous argillite	poor	rare sphaeromorphs	indeterminate
FCO02-03	586257	6563791	dark green shales interbedded with silt layers	n/a	abundant black and dark green crystals or various sizes, clays	indeterminate
FCO02-04	588164	6563785	brown mudstone intercalated within greywacke successions	n/a	silica fragments, clays, small-size dark crystals	indeterminate
FCO02-05	585873	6563191	mudstone interbedded with fine silts	n/a	silica fragments, abundant brown clays	indeterminate
FCO02-06	586673	6560580	fine siliceous silt	n/a	silica fragments, clays, sphaeromorphs, round quartz crystals	indeterminate
FCO02-07	586728	6560367	fine siliceous silt	n/a	black and dark green crystals or various sizes, silica fragments, clays	indeterminate
FCO02-08	599403	6557985	grey ribbon chert with abundant rads	moderate	<i>Plafkerium</i> sp., <i>Pseudostylosphaera magnispinosa</i> , <i>Triassocampe</i> sp., <i>Yeharaia elegans</i>	Middle Triassic; Anisian-early Ladinian
FCO02-09	599486	6557767	grey ribbon chert interbedded with siliceous argillite	poor	<i>Triassocampe</i> sp., pyrite crystals	Middle or Late Triassic
FCO02-11	599868	6557559	grey ribbon chert, small cliff	moderate	<i>Capnodocce</i> sp., <i>Canoptum</i> sp., <i>Sarla</i> sp.,	Late Triassic; late Carnian to Middle Norian
FCO02-12	600004	6557533	grey ribbon chert, 20 m above limestone unit	moderate	<i>Annulotriassocampe</i> sp., <i>Oertlispongos</i> sp., <i>Pseudostylosphaera</i> sp., <i>Triassocampe</i> sp.	Middle Triassic
FCO02-14a	600936	6559225	grey ribbon chert	moderate	<i>Capnodocce</i> sp., <i>Pachus</i> sp.	Late Triassic; late Carnian to Middle Norian
FCO02-14e	600936	6559225	grey ribbon chert	poor to mod	<i>Capnuhosphaera</i> sp., <i>Triassocampe</i> sp.	Late Triassic; Carnian to Middle Norian
FCO02-16	637657	6564355	black siliceous argillite	n/a	abundant clays, silica fragments	indeterminate
FCO02-20	637120	6564584	grey ribbon chert	moderate	<i>Latentifistula</i> sp., <i>Pseudoalibaillella scalprata</i>	Early Permian; Sakmarian-Kungurian
FCO02-21	637022	6564497	fine-grained volcaniclastics	n/a	abundant quartz crystals, some pyrite, silica fragments	indeterminate
FCO02-25	640120	6561340	grey ribbon chert	poor	<i>Eptingium</i> sp., <i>Pseudostylosphaera</i> sp., <i>Triassocampe</i> sp.	Middle Triassic
FCO02-27	640148	6561579	grey ribbon chert	poor	abundant spumellarians, some pyrite crystals	indeterminate

Table 1, continued

Station Number	NAD 83 UTM E	Zn8 UTM N	Lithology	Preservation	Radiolarian taxa Observations	Age
FCO02-29a	640014	6561937	black-grey ribbon chert unit (#1) within thick volcanoclastic unit	poor	<i>Oertlispongus</i> sp., <i>Pseudostylosphaera</i> sp., <i>Triassocampe</i> sp.	Middle Triassic
FCO02-29b	640014	6561937	black-grey ribbon chert unit (#1) within volcanoclastic unit	poor	<i>Triassocampe</i> sp., indeterminate spumellarians	Middle or Late Triassic
FCO02-30	640022	6561962	grey ribbon chert unit (#2) within volcanoclastic unit	poor	? <i>Plafkerium</i> sp., <i>Pseudostylosphaera</i> sp., <i>Triassocampe</i> sp.	Middle or Late Triassic
FCO02-32	639464	6562753	grey ribbon chert	poor	<i>Oertlispongus</i> sp., <i>Pseudostylosphaera</i> sp., <i>Triassocampe</i> sp., moderately abundant sponge spicules	Middle Triassic
FCO02-02-36	637908	6562716	grey ribbon chert	moderate	<i>Annulotriassocampe</i> sp., <i>Oertlispongus</i> sp., <i>Pseudostylosphaera nazarovi</i> , <i>Triassocampe</i> sp.	Middle or Late Triassic; late Ladinian-middle Carnian
JEN01-21-03	631724	6549334		poor	abundant recrystallized sphaeromorphs	indeterminate
JEN01-32-04a	646511	6569046		poor	sphaeromorphs, recrystallized spumellarians	indeterminate
JEN01-32-04b	646511	6569046		poor	sphaeromorphs, recrystallized spumellarians	indeterminate
JEN-02-33-03	642779	6569859	ribbon siliceous argillite	poor	Sphaeromorphs, probable spumellarians	indeterminate
KLA01-20-11	629542	6547894	see field notes	poor	<i>Plafkerium</i> sp.	Triassic
MMI01-08-05	637460	6563160	well-bedded black ribbon chert with continuous layers	poor to moderate	<i>Pseudostylosphaera</i> sp., narrow <i>Triassocampe</i> sp., <i>Yeharaia</i> sp.	Middle Triassic
MMI01-08-14	637613	6564455		poor	recrystallized sphaeromorphs, silica fragments	indeterminate
MMI01-13-11	642530	6567920		poor	abundant recrystallized silica rods (sponge spicules), black clays, sphaeromorphs	indeterminate
MMI01-13-12	642330	6567857		poor	sphaeromorphs, recrystallized spumellarians, sponge spicules, pyrite crystals	indeterminate
MMI01-14-03	640225	6567680	very well-bedded black and grey ribbon chert	poor	<i>Pseudostylosphaera</i> sp., narrow <i>Triassocampe</i> sp., recrystallized spumellarians	Middle Triassic
MMI01-14-04b	640150	6567736	tan and grey ribbon chert adjacent limestone conglom.	poor	<i>Entactinia</i> sp., <i>Quinqueremis</i> sp., <i>Pseudoalibaillella</i> sp. Cf. <i>lomentaria</i> , sponge spicules	Permian
MMI01-16-06*	639677	6567834	clast from polyimictic conglom.	poor	<i>Pseudostylosphaera</i> sp., narrow <i>Triassocampe</i> sp.	Middle Triassic
MMI01-19-09	630754	6542674	well-bedded black ribbon chert	good	<i>Entactinia</i> sp., <i>Latentifistula texana</i> , <i>Polyfistula</i> sp., <i>Pseudoalibaillella</i> sp. cf. <i>longicomis</i> , <i>Pseudoalibaillella lomentaria</i>	Early Permian
MMI01-20-08	632820	6550269	brown ribbon chert with very straight and consistent layers	good	<i>Canoptum</i> sp., <i>Capnuchosphaera</i> sp., <i>Capnodoce</i> sp.	Late Triassic, late Carnian-mid Norian
MMI01-29-02	622909	6554566	black ribbon chert, continuous bulbous beds	good	<i>Pseudostylosphaera compacta</i> , <i>Triassocampe</i> sp.	Middle Triassic
MMI01-29-04a	622901	6554125		poor	abundant sphaeromorphs	indeterminate
MMI01-29-04b	622901	6554125	pod in carbonaceous argillite matrix	poor to moderate	<i>Pseudoalibaillella lomentaria</i> , fragments of <i>Latentifistulidae</i>	Early Permian
MMI01-29-05a	622965	6554098		poor	rare sphaeromorphs, silica fragments, black clays	indeterminate
MMI01-29-05b	622965	6554098	semi-continuous black ribbon chert interlayered with wacke	poor	<i>Capnodoce</i> sp.	Late Triassic, late Carnian-mid Norian
MMI01-29-08	624533	6554045	Dark grey well bedded	moderate	abundant <i>Tritortis</i> sp., <i>Triassocampe</i> sp.	Middle Triassic
MMI01-30-05b	627060	6550890	Black massive to laminated chert	poor	<i>Entactinia</i> sp., ? <i>Pseudoalibaillella</i> , abundant sphaeromorphs	Paleozoic, possibly Permian
MMI01-30-08	626856	6550972	red rad chert with volcanoclastic	poor	? <i>Alibaillella</i> sp., abundant sponge spicules	possibly Paleozoic
MMI-02-11-04-1	627057	6550849	siliceous, fine-grained volcanoclastics	good	Rare so far	indeterminate
MMI-02-12-11	597476	6559246	grey ribbon chert	moderate	<i>Hegleria mamilla</i> , <i>Pseudoalibaillella</i> sp.	Middle Permian; Wordian-Capitanian

Table 1, continued

Station Number	NAD 83 UTM E	Zn8 UTM N	Lithology	Preservation	Radiolarian taxa Observations	Age
MMI-02-15-07-3	587129	6558441	siliceous, fine-grained volcaniclastics	moderate	? <i>Entactinosphaera</i> sp. cf. <i>sashidai</i> , ? <i>Parentactinia</i> sp., various forms of primitive ? <i>Pseudostylosphaera</i> sp., sponge spicules	possibly late Early Triassic or earliest Middle Triassic
MMI-02-28-10	592250	6568934	siliceous, fine-grained volcaniclastics	very poor	highly recrystallized elements, silica fragments, quartz crystals	indeterminate
MMI-02-30-09	624516	6566325	siliceous, fine-grained volcaniclastics	poor	abundant small-size spumellarians, clays	indeterminate
MMI-02-34-02-1*	621390	6543778	jasperoid radiolarian chert within pillow breccia unit	poor	<i>Entactinia</i> sp., ? <i>Follicucullus</i> sp., <i>Pseudoalibaillella</i> sp., <i>Latentibifistula</i> sp., fragments of <i>Latentifistulidae</i>	Permian
MMI-02-34-02-2*	621390	6543778	jasperoid radiolarian chert within pillow breccia unit	poor	Sphaeromorphs, probable spumellarians	indeterminate
MMI-02-34-07*	620383	6544147	10m x15m rusty black ribbon chert block above unconformity	moderate	<i>Eptingium</i> sp., <i>Pseudostylosphaera</i> sp. aff. <i>tenuis</i> , <i>Pseudostylosphaera coccostyla compacta</i> , <i>Triassocampe</i> sp., <i>Yeharaia</i> sp.	Middle Triassic, late Anisian or early Ladinian
YME01-23-03b	630968	6560595	silicified limestone (stratigraphic contact between pillows and limestone)		silica fragments	indeterminate

* as Station Number suffix indicates a sample from the Joss'alun discovery area, see Mihalyuk *et al.* (2003b, this volume)

ble size and range up to 1 m in long dimension. The unit may be repeated by a series of south-verging folds that have imparted a pervasive flattening fabric that dips moderately to the north. Structurally above the breccia are pillowed feldspar porphyry basalt flows (*see following*). The basalt-breccia contact is not exposed.

Breccia probably records tectonic instability of the Cache Creek chert-carbonate complex, possibly during off-scraping at an accretionary margin. Lack of evidence for rounding or sorting of clasts by alluvial processes argues against extensive subaerial exposure of the source area.

PORPHYRITIC FLOWS AND TUFF

Feldspar porphyry occurs both as pillowed flow and volcaniclastic facies less than 10m thick. Its contact with underlying limestone-chert breccia is not exposed, but it displays a slightly disrupted, probable stratigraphic contact with overlying well-bedded limestone having chert interlayers.

Porphyritic flows, together with under- and overlying units may be the stratigraphically equivalent to a succession in northwestern 104N/1 where mapping in 2002, revealed a highly indurated pyroxene-porphyritic flow unit at approximately the same stratigraphic interval, between a great thickness of chert and carbonate (Mihalyuk *et al.*, 2002), in the east-central part of the Blackcaps domain. Near treeline in "Laughing Moose Creek" valley, a sequence of chert, overlying breccia, and submarine pyroxene-porphyritic volcanic rocks may also be correlative. Magmagenesis of the augite-porphyritic unit displays a within-plate geochemical signature (English *et al.*, 2002).

It was probably formed in an ocean island or plateau setting. Chemical analysis of the feldspar porphyritic unit is pending. Age of the unit is not known. Interpillow lime mudstone and the overlying interbedded chert-limestone unit were both sampled for conodonts, but results were not available at the time of writing.

CARBONATE-DOMINATED STRATA

Carbonate rocks comprise much of the central part of the Nakina transect, here called the Sinwa domain (in the local Tlingit dialect "sinwa" means limestone). Most of the carbonate domain was mapped as part of the 2001 field program, with findings reported in Mihalyuk *et al.* (2002) and detailed in the M.Sc. thesis study by Merran (2002). In Late Carboniferous and Permian times (Table 2) these carbonate strata may have been deposited in a laterally extensive tract of shallow-water, massive limestone that interfingered with well-bedded lagoonal facies and talus to turbidite facies on the platform margins.

New observations, mainly from the Nakina River canyon and its tributaries, and from Mount Sinawa Eddy, are reported here.

NAKINA AND BRANCH CANYONS

Carbonate strata mapped within the Nakina River Canyon in northern 104N/2 are structurally interleaved with panels of ribbon chert 1 to 3 km thick (Figure 3). Various carbonate lithologies are well exposed. Most are the same or similar to units that have been previously reported (Mihalyuk *et al.*, 2002; Merran, 2002) from areas to the south and east. Typical lithologies include light grey, well-bedded, bioclastic (turbiditic?) limestone; coarse

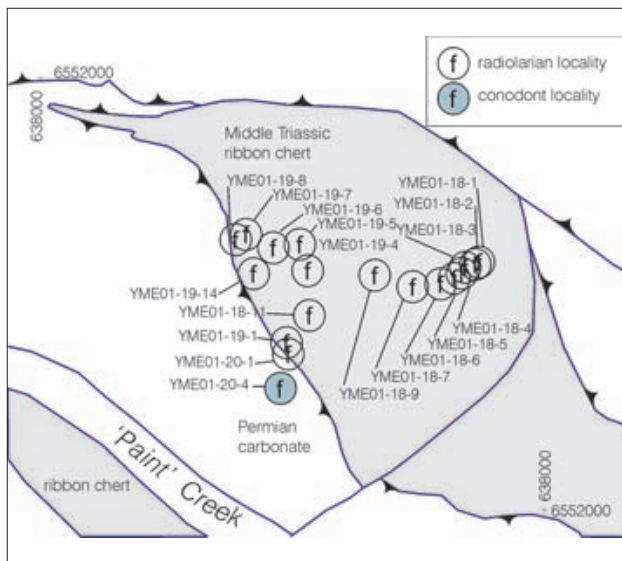


Figure 4. Major antiform north of Paint Creek is cored by Middle Triassic chert and overthrust by Permian carbonate. Fossil numbers prefixed by YME01 correspond with FCO01 prefix in Table 1.

limestone breccia which occurs as sheets and channels decimetres to several metres thick; indistinctly thick to medium-bedded, cream-coloured limestone about 80-120 m thick; and distinctly medium to thin-bedded, dark grey to black, fetid and/or argillaceous limestone ~40m thick. The latter two units are of particular note as they are primary constituents of a thrust-repeated section with a structural thickness of nearly 1 km (see Structural Styles, below).

Nakina River canyon in central 104N/2W, east and south of Sinawa Eddy Mountain, is precipitous. Observations of outcrops above the rim of the canyon and vantage point mapping of the canyon walls below, suggest that the dominant lithology is massive, very poorly bedded limestone, such as that which comprises the peak of Sinawa Eddy Mountain. However, a flight down the axis of this part of the canyon revealed moderately well-layered, thick to medium-bedded sections, commonly disrupted by complex subhorizontal faults and folds that mainly have <10m amplitudes and <100m wavelengths. Canyon walls provide the best exposures from which to gain an understanding of the details of the sedimentary and structural complexity of the Cache Creek within the Nakina Transect. Unfortunately, many parts of the main Nakina River canyon are difficult to access.

SINAWA EDDY

Massive limestone at Sinawa Eddy Mountain probably accumulated in an intra-oceanic platformal setting (Monger, 1975; Merran, 2002). Many cubic kilometres of this unit are featureless except for sparse crinoid ossicles and fragments of bivalves, bryozoa, rare corallites, pisoids or limestone clasts. In stark contrast, are well-bedded strata exposed along "Skull Creek" that incises the northern flanks of Sinawa Eddy Mountain. Most conspicuous is a ~40m thick succession of well-layered dark-coloured strata, including volcanic beds, between massive light grey limestone units. Contacts between beds are well exposed in

cliff-faces which are oriented perpendicular to the bedding. Only in such locations is it apparent that many of the contacts are either faults or sheared bedding planes. Nevertheless, the succession can be traced for about two kilometres across a shallow cirque. Part of this succession is in fault contact with the massive peak limestone (Photo 6). Exposed at the fault contact are vesicular, strongly fractured, rusty-weathering, dark green mafic flow rocks. They are cut by many high angle faults, making an estimation of thickness difficult. Overlying the mafic volcanics is about two metres of sooty limestone, which is also strongly faulted. This is in fault contact with beds of medium to dark grey limestone with thinner irregular layers of black chert. Bed thickness is variable, up to 1 m thick, but is typically 5 to 20 cm. Some of these beds (especially along strike to the north) contain silicified rugosan corals. The ?base of one bed is packed with 5-8 cm orbicular bivalves (Photo 7). In faulted (originally stratigraphic?) contact is a conspicuous 1-2m thick layer of red and green tuffite; in one place containing a 80cm thick limestone interbed. Very fine laminae display cross stratification and slump structures that suggest a north-dipping paleoslope (Photo 8). Northernmost



Photo 6. Well layered strata in fault contact with massive limestone that comprise the peak of Mt. Sinawa Eddy.



Photo 7. Articulated, orbicular bivalves are packed tightly at the base (?) of the limestone bed.

TABLE 2
FUSULINACEAN FORAM IDENTIFICATIONS
BY LIN RUI FROM SAMPLES COLLECTED WITHIN THE NAKINA TRANSECT

GSC Locality Number	BCGS Sample No.	UTM Coordinates (Zone 08V)	Fusulinacean Identification	Age
C220456	MMI01-20-4	631625E, 6550247N	<i>Sphaeroschwagerina</i> sp., <i>Triticites</i> sp., <i>Schwagerina</i> sp.	Early Permian, Asselian
C220457	MMI01-20-6	632197E, 6550113N	<i>Schwagerina</i> sp.	Late Carboniferous-Early Permian
C220460	MMI01-21-5	632255E, 6548980N	<i>Schubertella</i> sp., <i>Daixina</i> sp.	Late Carboniferous-Early Permian
C220461	MMI01-21-6	632268E, 6549033N	<i>Sphaeroschwagerina</i> sp., <i>Schwagerina</i> sp.	Early Permian, Asselian
C220462	MMI01-21-7	632305E, 6549191N	<i>Sphaeroschwagerina</i> sp., <i>Triticites</i> sp., <i>Schwagerina</i> sp.	Early Permian, Asselian
C220462	MMI01-21-7B	632305E, 6549191N	<i>Sphaeroschwagerina</i> sp., <i>Triticites</i> sp.	Early Permian, Asselian
C220463	MMI01-21-8B	632352E, 6549607N	? <i>Eostaffellina</i> sp., ? <i>Eoschubertella</i> sp.	Middle Carboniferous, Moscovian
C220464	MMI01-21-9C	632326E, 6549629N	<i>Mediocris</i> sp., <i>Eoschubertella</i> sp., ? <i>Profusulinella</i> sp.	Middle Carboniferous, Moscovian
C220464	MMI01-21-9D	632326E, 6549629N	? <i>Pseudostaffella</i> sp., <i>Profusulinella</i> sp.	Middle Carboniferous, Moscovian
C220465	MMI01-23-11	641824E, 6559764N	<i>Parafusulina</i> sp., <i>Pseudodoliolina</i> sp.	Middle Permian, Roadian (Kubergandian)
C220466	MMI01-23-12	641306E, 6559781N	<i>Pseudoendothyra</i> sp., <i>Schubertella</i> sp.	Early Permian-Middle Permian
C220467	MMI01-23-13	641176E, 6559686N	<i>Schubertella</i> sp., ? <i>Schwagerina</i> sp.	Early Permian-Middle Permian
C220468	MMI01-28-8D	654178E, 6564091N	<i>Schubertella</i> sp.	Early Permian-Middle Permian
C220469	MMI01-29-1A	622764E, 6554988N	<i>Parafusulina</i> sp.	Permian, Leonardian-Rodian
C220469	MMI01-29-1B	622764E, 6554988N	<i>Parafusulina</i> sp.	Permian, Leonardian-Rodian
C220499	MMI01-29-18	625936E, 6552249N	<i>Parafusulina</i> sp.	Permian, Leonardian-Rodian
C220470	MMI01-30-6C	626779E, 6551009N	No fusulinaceans were found in this sample	
C220470	MMI01-30-6D	626779E, 6551009N	? <i>Schubertella</i> sp.	?Permian
C220472	MMI01-31-11A	622642E, 6553662N	<i>Colania</i> sp.	Middle Permian, Wordian
C220472	MMI01-31-11B	622642E, 6553662N	<i>Colania</i> sp.	Middle Permian, Wordian
C220472	MMI01-31-11C	622642E, 6553662N	<i>Schubertella</i> sp., <i>Nodosaria</i> sp., <i>Pachyphloia</i> sp.	Middle Permian, Wordian
C220473	MMI01-31-12A	622600E, 6553670N	<i>Schwagerina</i> sp.	Middle Permian, Wordian
C220473	MMI01-31-12G	622600E, 6553670N	? <i>Schubertella</i> sp., ? <i>Schwagerina</i> sp.	Middle Permian, Wordian
C220475	MMI01-31-14A	622580E, 6553695N	<i>Colania</i> sp.	Middle Permian, Wordian
C220475	MMI01-31-14E	622580E, 6553695N	<i>Schwagerina</i> sp.	Middle Permian, Wordian

TABLE 3
PRODUCTIVE CONODONT SAMPLES COLLECTED FROM THE CACHE CREEK COMPLEX
DURING THE 2001 FIELD SEASON (36 SAMPLES, 9 PRODUCTIVE)¹

Field Number	UTM east	UTM north	GSC number	Fossils	Preservation	CAI	Age & comments
FDE01-16-5,	622689	6564368	C-306173	undiagnostic ramiform elements	poor	5	probably Triassic
YME01-16-6	620615	6558443	C-306178	<i>Neogondolella inclinata</i> together with <i>Metapolygnathus polygnathiformis</i>	poor	5	Ladinian-early Carnian (M-Late Triassic)
YME01-19-11	633081	6555787	C-306186	<i>Neogondolella szaboi</i>	poor	5	Anisian (Middle Triassic)
YME01-20-4	633980	6553859	C-306187	<i>Sweetognathus</i> ? and <i>Hindeodus</i> ? occur together with indeterminate ellisonids	very poor	5-5.5	Permian
YME01-21-6	632100	6560081	C-306189	<i>Sweetognathus</i> ? and <i>Hindeodus</i> ? occur together with indeterminate ellisonids	very poor	5-5.5	Permian
YME01-22-9	630381	6560265		undiagnostic ramiform elements	poor	5	probably Triassic
YME01-23-3	630968	6560595	C-306191	<i>Idiognathoides</i> sp. and <i>Neognathodus</i> ? sp.	very poor	5.5-6	probable Bashkirian to Moscovian (Late Carboniferous) ²
YME01-24-1	647466	6554472	C-306192	<i>Sweetognathus</i> ? and <i>Hindeodus</i> ? occur together with indeterminate ellisonids	very poor	5-6	Permian
YME01-31-7	637065	6550442	C-306195	undiagnostic ramiform elements	poor	5	probably Triassic

¹ Identifications by M. Orchard, Geological Survey of Canada

² In Nechako region they characterize the first major carbonate (Orchard *et al.*, 2001)

outcrops of this unit are very different in character. They are dun-weathering calcareous volcanic sandstone (Photo 9a), commonly containing decimetre angular blocks of fine-grained carbonate (Photo 9b). Trough cross stratification indicates paleoflow to the south, opposite to paleoflow in the red tuffite. Dun volcanic sandstone is apparently conformably overlain by light grey, poorly layered, thick-bedded limestone, which becomes massive 5-20 metres up section. In one place, at or near the upper volcanic sandstone contact, a breccia with clasts up to the size of small rooms, occurs near the base of the massive unit (Photo 10a). Other such breccia zones can be mapped within the massive unit. They may be collapse breccias related to tectonism.

On the ridge east of `Skull Creek` a similar coarse breccia apparently grades laterally into a homogeneous breccia with pebble-sized clasts of limestone, sparse chert and rare, ochre tuff clasts, forming a persistent layer up to 20 m thick (Photo 10b). In places the breccia is well bedded and graded, but more commonly it is massive. This unit is apparently in the immediate hangingwall of a gently west-dipping thrust that most commonly juxtaposes the light grey, massive carbonate with more steeply dipping, well-bedded, dark grey carbonate. The pebble breccia may represent a synorogenic clastic wedge that is overridden by the massive carbonate. A similar unit of possibly synorogenic breccia was mapped between the thick chert unit and well-bedded carbonate in northern 104N/2E.

FELSIC VOLCANIC AND INTERCALATED UNITS

Mapping in 2001 identified bimodal volcanic rocks within a package of dominantly Middle Triassic chert (Figure 3; Mihalynuk *et al.*, 2002). Mapping in 2002 traced the felsic volcanic unit and associated thinly-bedded, platy limestone across the alpine ridges between the lower stretches of `Paint` and Horsefeed creeks. This interval can



Photo 8. Cross stratified tuffite indicates northward paleoflow.

be followed for ~800 m before it is lost beneath cover in a tributary valley of Horsefeed Creek. An exposure of coarse, feldspar-phyric breccia of probable intermediate composition crops out ~600m to the west.

Felsic tuffite forms beds centimetres to decimetres thick. Reworked volcanic detritus, including euhedral quartz grains, are intercalated with green and maroon chert that contains radiolaria of “Paleozoic, possibly Permian” age and abundant sponge spicules (Table 1, MMI01-30-5b). Additional microfossil age determinations are pending. A U-Pb age determination of a sample of quartz-phyric tuff is also pending. Reworked fusulinaceans from the platey limestone are “?Permian” (Table 2, MMI01-30-6D). Two conodont samples collected from sooty limestone were barren. Along strike to the southeast, chert structurally above the volcanic unit contain Middle Triassic radiolaria (FCO01-17-5 to 14, 9 samples; Table 1). The age of the volcanic strata is most likely Permian to Middle Triassic. Volcanic rocks of the Kutcho Formation and associated massive sulphide mineralization were deposited within this time interval (241 - 253 Ma; Childe and Thompson, 1997). Coarse, euhedral quartz phenocrysts are also a characteristic of the Kutcho Formation. Based on these criteria a tenuous correlation with the mineralized Kutcho Formation is suggested. Elevated base metal values in the RGS survey results (Jackaman, 2000) further points to potential for mineralization in the drainage basins where this stratigraphy occurs (*c.f.* Mihalynuk *et al.*, 2002). However, a re-evaluation in 2002 detected no sign of base metal sulphide mineralization in association with the felsic tuff.

COARSE CLASTIC UNIT

Coarse, polymictic conglomerate are known from three separate localities. Two isolated areas are southeast of Mt. O’Keefe where their area of exposure totals less than ~0.2 km². A more widespread unit north of Hardluck Peaks crops out across an area of ~4.5 km². In all areas the unit appears to rest atop mafic volcanoclastic strata. Clasts include granitoid boulders as well as other clasts that are derived

lithologies within the Cache Creek complex: chert, mafic volcanics, limestone, and ultramafite (in order of decreasing abundance). Near Hardluck Peaks, chert blocks range up to the size of small houses, probably deposited as landslide debris near a fault scarp. Middle Triassic radiolaria collected from one such block provide a Middle Triassic maximum age for deposition of that part of the unit (*see* Mihalynuk *et al.*, 2003, this volume).

LATE TRIASSIC TO EARLY JURASSIC CACHE CREEK WACKE

Wacke of the Cache Creek complex was divided into two main units by Mihalynuk *et al.* (2002): a common variety comprised largely of a siliceous mud matrix (a clastic-rich variant of Type 4a chert), and less common variety that is mainly silt and sand-sized grains. Similar relative abundances of these units are mapped in the western Nakina transect. Siliceous mud-rich wacke is brown and less commonly dark grey, black or blue-grey. It commonly contains chert grains and rare cobbles, and volcanic clasts from ash to lapilli size. Rare quartz grains may be derived from quartz diorite, which occurs as, foliated granules. Locally, the unit grades into chert or volcanoclastic rocks. Where this occurs near ‘Blackcaps Mountain’ the chert is of Middle or Late Triassic age (Table 1).



Photo 9. (a) Distinctive, dun-weathering, volcanoclastic limestone. (b) Angular limestone blocks of boulder size indicate high energy, rapid deposition.



Photo 10. (a) Coarse breccia within otherwise massive light grey limestone. (b) Laterally persistent limestone pebble breccia is remarkably uniform in character.

Sand or silt-sized grains are common within some wacke beds; however, quartz grains locally comprise a significant proportion of the beds. Three of these areas are described in Mihalynuk *et al.* (2002). They are on the north flank of `Scarface Mountain`, on the western ridge of Mount Nimbus, and between lower Horsefeed and `Paint` creeks. At these localities, monocrystalline quartz can comprise as much as 20-30% of the grains.

At `Scarface Mountain,, a chert-dominated fault panel was described by Mihalynuk *et al.* (2002) as containing between 1 and 3 metres of well-bedded, coarse, olive coloured, quartz-rich volcanic sandstone that caps a section of basalt flows and conformably overlying corals within a carbonate buildup about 18m thick. These authors suggested that the clastic rocks smothered the corals, but this interpretation is not supported by new age data. Preliminary fossil identification of the reef fauna indicates a probable Early Carboniferous age, probably late Tournaisian or Early Viséan, according to W. Bamber at the Geological Survey of Canada (personal communication, 2002); whereas, detrital zircons from the overlying wacke are as young as Early Jurassic (*see* Isotopic Age Determinations). A major hiatus is indicated.

West of Mount Nimbus, thinly bedded, silty wacke comprises a 5 to 20+m thick fault-bounded panel between kilometre-thick panels of mafic volcanic and carbonate rocks. Thin beds and lamellae have been strongly disrupted

by synsedimentary micro-faults. Populations of detrital zircons extracted from this unit are Middle to Late Triassic in age (Devine, 2002). An adjacent succession of cherty argillite and ribbon chert displays very consistent, straight layering (Type 3 chert). It is brown weathering, and contains Late Triassic radiolaria (MMI01-20-8; Table 1).

Between lower Horsefeed and `Paint` creeks, fault-bounded panels of quartz-rich wacke are tectonically interleaved chert and lesser carbonate. Fault panels are a few metres to a few hundred metres in thickness, and display abundant evidence for soft-sediment deformation. Middle Triassic radiolaria were extracted from a carbonaceous cherty argillite unit (MMI01-29-2), which is concordant with adjacent carbonate containing Leonardian-Roadian fusulinids (Early-Middle Permian; MMI01-29-1A, 1B; Table 2). Approximately 1km away, across strike, is a disrupted argillaceous chert unit containing semi-continuous beds and bulbous layers of chert. Radiolaria extracted from the latter (MMI01-29-4b, Table 1) reveal an Early Permian age. These beds are presumably in thrust contact with ribbon chert and quartz-bearing wacke. Radiolarian chert occurs within the wacke as subangular blocks and semi-continuous beds up to 30 cm thick. Radiolaria from one block returned a Late Triassic age (MMI01-29-5b, Table 1), one of the youngest ages obtained from chert of the Cache Creek complex. Farther across strike, in another fault panel, ribbon chert from a locality with unusually straight beds (Type 3 chert), contain Middle Triassic radiolaria (MMI01-29-8).

LABERGE GROUP

Laberge Group is restricted to the western end of the Nakina transect, west of the Nahlin Fault (Figure 3). Laberge group stratigraphy within the transect area, together with a preliminary assessment of its hydrocarbon potential, is presented by English *et al.* (2003, this volume). Here we outline only observations that are not included by those authors.

CHERT PEBBLE CONGLOMERATE

Chert pebble conglomerate is known from immediately southwest of the Nahlin Fault along the informally named `Psychobear` ridge. A resistant band of listwanite along the Nahlin fault forms the ridge crest and conglomerate is exposed in a series of low outcrops covering about 100 m² within open forest just a few metres west of the ridge crest (southeast of Goldbottom Creek, too small to show on Figure 3). Chert pebbles are well-rounded, dominantly grey in colour and comprise about 80% of the unit.

This unit is tentatively correlated with Middle Jurassic (Bajocian) chert pebble conglomerate known from the Tulsequah area (Mihalynuk *et al.*, 1995).

MAGNETIC GARNET-OLIVINE WACKE

A distinctive wacke unit within the Laberge Group contains up to 3% detrital garnet and sparse, very fresh olivine grains (Photo 11). Plagioclase-hornblende porphyry

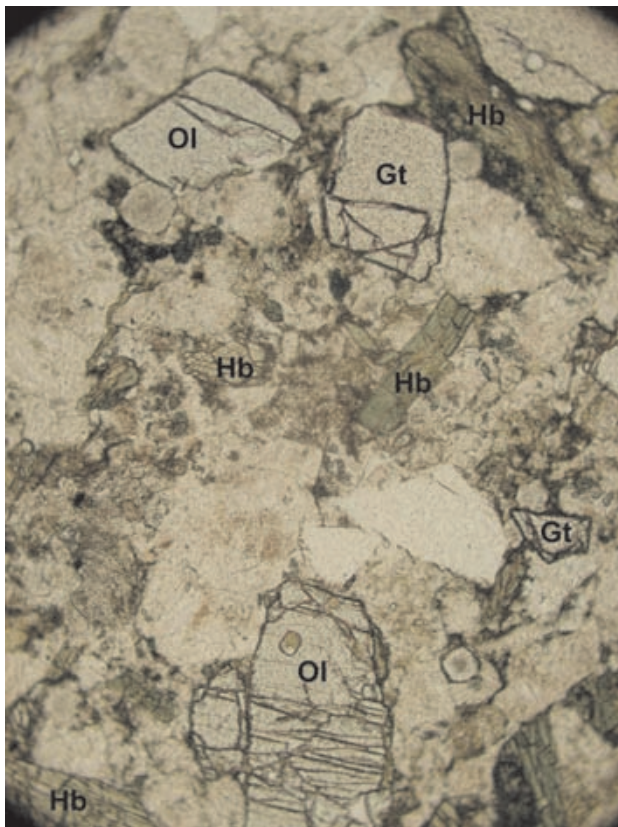


Photo 11. Garnet (Gt), fresh olivine (Ol) and hornblende (Hb) within magnetic, tuffaceous wacke of the Laberge Group. Length of photo represents ~2mm.

clasts of sand to pebble size are common. The unit is abnormally magnetic ($15\text{-}22 \times 10^{-3}$ SI) and correlates with magnetic anomaly that is well portrayed on the regional aeromagnetic survey map (Dumont *et al.*, 2001c). It is one of the few marker units within the Laberge Group of the Nakina transect and has been sampled for detrital zircon separation and dating in order to help constrain its maximum age. Microprobe analyses of the garnet and olivine grains are in progress.

SLOKO VOLCANIC STRATA

Mafic to felsic continental arc volcanic rocks of the Sloko Group are restricted to the western margin of the transect area. Common units include white and rust felsic tuff, green lapilli tuff and coarse breccia, and dense, feldspar-phyric flows and sills. Unconformable or fault contacts with the Laberge Group strata are well exposed. A basal conglomerate is locally well developed. South of Paradise Peak, the basal conglomerate unit is more than 30 metres thick (Photo 12). Throughout the lower half of the unit are seams of coal up to 15cm thick. Some seams are relatively pure. More commonly, they have a significant ash component. Clasts within the conglomerate are mainly derived from the Sloko Group or the Laberge Group strata.

Polymictic ash tuff is a common constituent within the lower Sloko Group. Pyroclasts are commonly light green



Photo 12. Basal conglomerate of the Sloko Group south of Paradise Peak, contains coal seams, especially in its lower half.

lapilli, but range to dark-coloured bombs up to a metre or more across (Photo 13). Another common lithology is cream coloured lapilli and ash tuff with local rust weathering.

Dense, dark green to black, feldspar-porphyrific flows and sills are minor constituents within the volcanic stratigraphy, except for where they crop out west of Pike Lake. At this locality, fresh basalt is tentatively included with the Sloko Group as originally suggested by Aitken (1959) because it appears to be much less altered than basaltic rocks

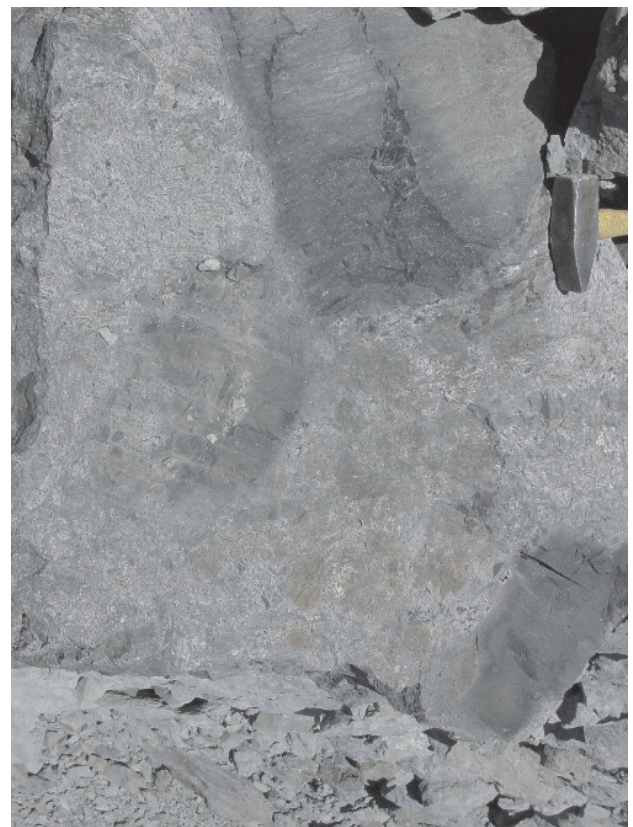


Photo 13. Coarse angular bombs in Sloko Group pyroclastic unit, note sledge head for scale.

of the Cache Creek complex. However, the unit displays a magnetic character indistinguishable from the adjacent Cache Creek complex, and like the older units, it is also truncated by the Nahlin fault.

LATE SYN- TO POST-ACCRETIONARY INTRUSIVE ROCKS

Three semicircular to elongate intrusions lie northeast of the Nahlin fault. All are composed of hornblende > biotite granodiorite and quartz diorite. Internal schlieren or contact zones of quartz diorite are common. Aitken (1959) mapped them as Middle Jurassic age. All major bodies have been sampled for isotopic age determinations, but at the time of writing, only the Nakina River stock age has a confirmed Middle Jurassic age by $^{40}\text{Ar}/^{39}\text{Ar}$ dating of biotite (see Mihalyuk *et al.*, 2003 in the following paper).

Nakina River stock (named by Aitken, 1959) is the largest and most elongated, with its long axis oriented parallel to the regional structural grain. It extends ~18 km from south of the Atlin 104N map area to the southern flank of Focus Mountain. Within the map area, it averages about 4 km across.

In northeastern 104N/3, the Chickoida Mountain stock (Aitken, 1959) is a composite body that is slightly east-northeast elongated, with maximum continuously exposed dimension of 7.5 km. However, outcrops up to 2.5 km west of the continuous exposures of the body appear from a distance to also be intrusive. It is about 4 km wide, although discontinuous outcrops on its treed northern slope probably belong to an apophysis that extends a further 2 km from the main body. An annular positive magnetic anomaly that occupies the centre third of the stock may be a late intrusive phase. However, an isolated occurrence (~2 Ha) of Quaternary basalt with abundant mantle xenoliths occurs on the inner margin of the anomaly annulus.

A small, ~1km² granodioritic body centred 3.5 km east-southeast of Focus Mountain, had not been previously mapped. It is herein called the Focus Mountain stock.

All intrusive bodies cut across pre-existing structures, but also appear to have intruded with a force that has shouldered aside and warped structural trends in the country rocks. Such relationships are well described by Aitken (1959) and are the subject of detailed mapping and petrographic studies by Bath (2003, this volume).

SLOKO DIORITE

A subcircular diorite stock underlies the precipitous terrain around Paradise Peak. It intrudes and thermally alters both Laberge Group and Sloko Group strata. Like other Sloko suite intrusive bodies, this stock is believed to be broadly comagmatic with the volcanic carapace into which it intruded.

ISOTOPIC AGE DETERMINATIONS

We report here on successful $^{40}\text{Ar}/^{39}\text{Ar}$ age dating of the mafic oceanic crustal rocks and detrital zircon age de-

terminations from overlying coarse clastic strata. No age determination of the mantle rocks has yet been attempted from the Cache Creek in the Nakina transect, primarily because harzburgite normally lacks mineral species that are amenable to conventional dating techniques. However, Gordey *et al.* (1998) were apparently successful in recovering a small amount of broken, clear, colourless zircon from peridotite in the Teslin map area. They reported an age 245.4 +/-0.8 Ma and interpret it as the age of uplift and quenching of the mantle, possibly a few million years after being brought to the surface by sea floor spreading.

PROCEDURES FOR $^{40}\text{Ar}/^{39}\text{Ar}$ ANALYSIS

Laser $^{40}\text{Ar}/^{39}\text{Ar}$ step-heating analysis was carried out at the Geological Survey of Canada laboratories in Ottawa, Ontario. Selected samples were processed for $^{40}\text{Ar}/^{39}\text{Ar}$ analysis of hornblende phenocrysts by standard heavy-liquid mineral separation techniques, followed by hand-picking of clear, unaltered crystals in the size range 0.5 to 1 mm. Individual mineral separates were loaded into aluminum foil packets along with a single grain of Fish Canyon Tuff Sanidine (FCT-SAN) to act as flux monitor (apparent age = 28.03 ± 0.1 Ma; Renne *et al.*, 1994). The sample packets were arranged radially inside an aluminum can. The samples were then irradiated for 12 hours at the research reactor of McMaster University in a fast neutron flux of approximately 3 × 10¹⁶ neutrons/cm². Neutron flux gradients throughout the sample canister were evaluated by analyzing the sanidine flux monitors included with each sample packet. We then interpolated a linear fit for calculated J-factor versus sample position. The error on individual J-factor values is conservatively estimated at ±1.0% (2 sigma).

Upon return from the reactor, samples were split into several aliquots and loaded into individual 1.5 mm-diameter holes in a copper planchet. The planchet was then placed in the extraction line and the system was evacuated. Heating of individual sample aliquots in steps of increasing temperature was achieved using a Merchantek MIR10 10W CO₂ laser equipped with a 2 mm x 2 mm flat-field lens. The released Ar gas was cleaned over getters for ten minutes, and then analyzed isotopically using the secondary electron multiplier system of a VG3600 gas source mass spectrometer; details of data collection protocols can be found in Villeneuve and MacIntyre (1997) and Villeneuve *et al.* (2000).

Corrected argon isotopic data are listed in Table 4, and presented as gas release spectra shown on Figure 5. Such plots provide a visual image of replicated heating profiles, relative gas volumes per heating step, evidence for Ar-loss in the low temperature steps, and the error and apparent age of each step.

Because the error associated with the J-factor is systematic and not related to individual analyses, correction for this uncertainty is not applied until calculation of dates from isotopic correlation diagrams (Roddick, 1988). No evidence for excess ^{40}Ar was observed in any of the samples and, therefore, all regressions are assumed to pass through

the $^{40}\text{Ar}/^{36}\text{Ar}$ value for atmospheric air (295.5). All errors are quoted at the 2 sigma level of uncertainty.

PROCEDURES FOR U/PB ANALYSIS

Following the separation of heavy minerals using heavy liquids, samples were passed through a Frantz LB-1[™] magnetic separator to purify zircon, titanite and monazite. Zircon crystals were selected for analysis based on criteria that optimized for their clarity, lack of cloudiness and colour, and lack of fractures. All zircons were abraded prior to analysis to increase concordance by removing the outer portions of the grains where much of the Pb-loss and alteration take place (Krough, 1982).

Following abrasion, photography, and final mineral selection, mineral fractions were analysed according to methods summarised in (Parrish *et al.*, 1987). Data have been reduced and errors have been propagated using software written by J. C. Roddick; error propagation was done by numerical methods (Parrish *et al.*, 1987; Roddick, 1987). Error ellipses on concordia diagrams are shown at the 2-sigma (95% confidence) level of uncertainty. Final errors are indicated on Table 5. Fraction letters shown on concordia diagrams are keyed to the fraction letters in Table 5.

AGE OF OCEANIC CRUSTAL ROCKS

Of all magmatic rocks sampled within the Nakina transect, the contacts between the Tseta Creek plagiogranite and mafic volcanic and diabasic rocks that it intrudes has been least affected by faulting. Dating of the Tseta Creek plagiogranite by both $^{40}\text{Ar}/^{39}\text{Ar}$ and U-Pb age methods at the GSC's Geochronology Laboratory in Ottawa yielded ages that compare favourably despite problems with $^{40}\text{Ar}/^{39}\text{Ar}$ determination of hornblende due to a

high Ca/K ratio (>70), and abundant Cl_2 , leading to larger than typical uncertainties (Table 4, Figure 5). A second of two Ar analyses produced a preferred $^{40}\text{Ar}/^{39}\text{Ar}$ age of 265 ± 18 Ma, as determined from a plateau representing 98% of Ar released.

Abundant, high quality zircons were recovered from the plagiogranite. Four concordant to near concordant, overlapping analyses result in an interpreted age of 261.4 ± 0.3 Ma, with MSWD of 0.6 (Table 5, Figure 6). This is the oldest directly dated oceanic crust in the northern Cache Creek terrane and is coeval with a 263.1 ± 1.4 Ma age determination (Mihalynuk *et al.*, 1999) from submarine ignimbrite in the French Range (Figure 1). The crustal age data are corroborated by unpublished age data from knockers near Mount Nimbus (located in NTS104N/1), which also returned Late Permian ages as reported by Devine (2002).

QUARTZ-RICH CLASTIC ROCKS

Quartz-rich strata were sampled at two localities for detrital zircon age determinations. Two samples were collected from an olive green, quartz-rich sandstone that overlies fossiliferous limestone interbedded with mafic tuff on the north side of 'Scarface Mountain'.

Seven samples were collected from a succession of immature, quartz-rich clastic rocks that unconformably overlies the oceanic crustal section north of Hardluck Peaks (above the Joss'alun occurrence, *see* Mihalynuk *et al.*, 2003, this volume). One sample was collected from coarse sandstone, and six granitoid boulders were taken from a very coarse conglomerate.

Zircons were extracted and single zircon grains were analysed by the SHRIMP (Super High Resolution Ion

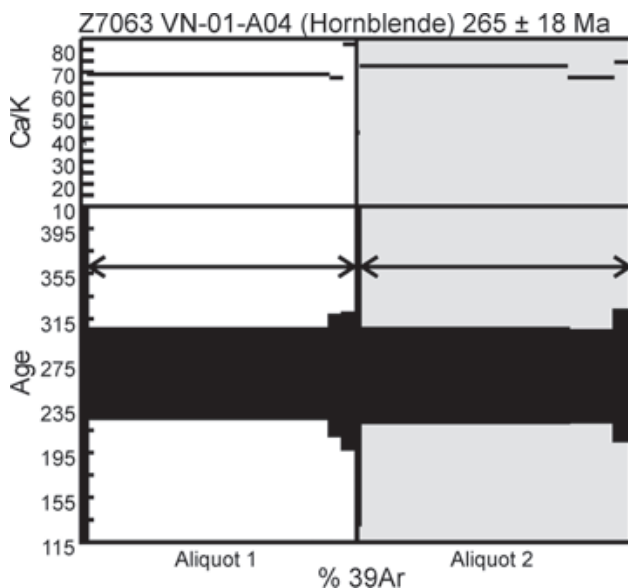


Figure 5. Stepwise heating and $^{40}\text{Ar}/^{39}\text{Ar}$ release spectrum for hornblende from the Tseta Creek plagiogranite.

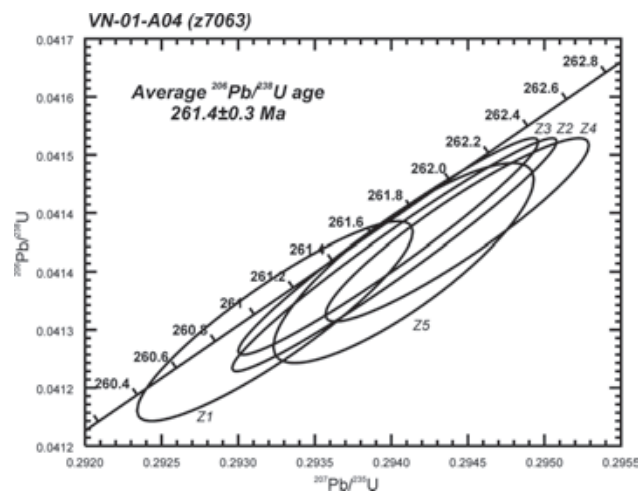


Figure 6. Concordia plot of U-Pb isotopic composition of zircon populations extracted from the Tseta Creek plagiogranite. A weighted average of four concordant fractions yields a best interpreted age of 261.4 ± 0.3 Ma.

TABLE 4
⁴⁰Ar/³⁹Ar ISOTOPIC DATA FROM A HORNBLENDE SEPARATE OF THE
TSETA CREEK PLAGIOGRANITE

P ^a Volume x10 ⁻¹¹ cc	³⁹ Ar	³⁶ Ar/ ³⁹ Ar	³⁷ Ar/ ³⁹ Ar	³⁸ Ar/ ³⁹ Ar	⁴⁰ Ar/ ³⁹ Ar	% ⁴⁰ Ar ATM	* ⁴⁰ Ar/ ³⁹ Ar	f ₃₉ ^b (%)	Apparent Age Ma ^c
VN-01-A04 Hornblende; J=.01442060 (Z7063; 59.0116°N 132.2279°E)									
<i>Aliquot: A</i>									
2.4	0.0057	1.9490±0.4669	8.452±1.799	1.049±0.264	592.475±125.204	97.3	16.278±62.523	0.1	380.40±1364.39
3.0	0.0152	0.7524±0.1102	10.726±1.109	0.695±0.116	235.395±26.519	94.5	12.895±23.268	0.2	307.68±513.05
3.9	0.0133	0.5484±0.0980	13.460±1.082	0.410±0.076	173.264±19.578	93.7	10.972±26.352	0.2	265.00±595.92
4.6	0.0239	0.5754±0.0711	20.308±1.870	0.466±0.047	181.714±18.252	93.6	11.566±14.132	0.3	278.28±315.67
5.0	0.0124	0.3688±0.1477	19.642±2.690	0.270±0.119	119.868±23.268	91.1	10.610±40.696	0.2	256.84±938.26
5.5	0.0195	0.2121±0.0535	24.337±1.669	0.265±0.076	73.796±11.720	85.2	10.950±15.326	0.3	264.51±345.01
6.0	3.6095	0.0084±0.0008	35.553±0.189	0.180±0.011	13.506±0.132	18.5	11.011±1.778	49.6	265.87±39.92
6.5	0.1965	0.0082±0.0052	34.762±0.939	0.191±0.012	13.384±1.214	18.3	10.937±2.384	2.7	264.21±53.57
12.0	0.203	0.0084±0.0056	42.453±0.771	0.201±0.021	13.220±1.029	19	10.711±2.684	2.8	259.12±60.50
<i>Aliquot: B</i>									
2.4	0.0121	1.0745±0.1481	8.718±1.263	1.360±0.139	335.409±32.814	94.7	17.709±33.660	0.2	410.30±705.20
3.9	0.0253	0.5771±0.0558	22.097±1.583	0.620±0.058	187.900±13.526	90.8	17.262±12.956	0.4	401.01±270.24
5.5	2.4036	0.0048±0.0006	37.425±0.367	0.196±0.011	12.356±0.136	11.5	10.939±1.863	33	264.25±41.87
6.0	0.5395	0.0003±0.0018	34.808±0.356	0.171±0.015	10.984±0.385	0.8	10.900±1.807	7.4	263.39±40.63
12.0	0.2034	0.0042±0.0059	38.325±0.905	0.185±0.013	12.200±1.037	10.4	10.929±2.588	2.8	264.02±58.17
3.9	16.336	0.1111±0.0017	0.025±0.001	0.121±0.011	33.074±0.081	99.3	0.245±0.492	8.4	1.41±2.84
4.2	8.4777	0.0815±0.0003	0.025±0.001	0.115±0.011	24.358±0.089	98.9	0.267±0.063	4.3	1.54±0.37
4.6	8.2439	0.0763±0.0003	0.024±0.001	0.111±0.011	22.793±0.076	98.9	0.261±0.090	4.2	1.50±0.52
5.5	10.2597	0.0714±0.0003	0.021±0.001	0.103±0.011	21.333±0.088	98.8	0.250±0.071	5.2	1.44±0.41
6.5	17.7946	0.0688±0.0004	0.020±0.001	0.104±0.011	20.606±0.072	98.7	0.265±0.097	9.1	1.53±0.56

a: Power # as measured by laser in % of full nominal power (10W)

b: Fraction ³⁹Ar as percent of total run

c: Errors are analytical only and do not reflect error in irradiation parameter J

d: Nominal J, referenced to FCT-SAN=28.03 Ma (Renne *et al.*, 1994)

∅ All uncertainties quoted at 2 level

MicroProbe) at the Geological Survey of Canada in Ottawa (for methodology see Mihalynuk *et al.*, 2003, this volume).

Analysis of one of the 'Scarface Mountain' sandstone samples revealed a bimodal age population. Preliminary age determinations show dominance by a population with ages falling between 331±15 Ma to 362±15 Ma, based upon concordant to near concordant ²⁰⁶Pb/²³⁸U ages. A single Jurassic age of 182±4 Ma represents a lone outlier from this age range. Based only on these ages, the (currently) nearest source terrains are either Stikine or Quesnel arc rocks (or their metamorphosed equivalents, which together with pericratonic strata, comprise the Yukon-Tanana terrane). If the source is one of these, it is necessary to explain the lack of Late Triassic zircons because magmatic rocks of Late Triassic age are known within both Stikine and Quesnel arcs (Figure 1, inset), especially in their southern parts. In the northern parts of these arc terranes, quartz-bearing igneous rocks of Late Triassic occur as granitic to granodioritic plutonic roots of the Stuhini arc (*e.g.* Mihalynuk, 1999; Hart *et al.*, 1995) and are common detritus in the early Jurassic Laberge Group; whereas, quartz-bearing magmatic rocks of similar age are rare in northern Quesnel terrane. Consequently, northern Quesnel arc may be the most likely source of the detritus. A lack of preCambrian zircons excludes YTT as a likely source.

Analysis of the Joss'alun sandstone sample (VN-01-A03) reveals a surprising homogeneity of detrital zircon ages; all are Late Permian to earliest Triassic (based on time scale of Okulitch, 1999). Analyses of zircons extracted from granitoid boulders from within the same clastic succession are pending. For more information on the Joss'alun sandstone and corroborating microfossil age determinations, see Mihalynuk *et al.* (2003, this volume).

STRUCTURAL STYLES

Domains shown on Figure 2 are largely based on changes in structural style. A most profound control on structure and distribution of different rock types is the Nahlin fault, which separates mantle tectonite and accretionary mélangé of the Cache Creek complex, from Lower to Middle Jurassic Laberge Group strata. Laberge Group strata are deformed in a southwest-verging fold and thrust belt.

Many parts of the Nakina transect are so intensely deformed that structural complexity must be portrayed schematically, at scales of 1:50 000 or smaller. Thus, previous maps (*i.e.* Aitken, 1959; Monger, 1975), as well as that shown in Figure 3, under-represent structural complexity. Our mapping at 1:20 000 scale, compiled at 1:50 000, and further simplified on Figure 3 (about 1:250 000) is of suffi-

cient detail to show several structural features not reported prior to the Nakina transect mapping.

A general northwest structural fabric parallels the Nahlin ultramafic body and the Nahlin fault, although local trends can change direction radically. For example, a south-verging fold and thrust belt occupies northeastern 104N/2.

Other structural features of note are:

- a northeast-trending belt of intense thrust imbrication north of Nakina River in north-central 104N/2.
- northwest-trending, high angle faults, potentially of crustal-scale, offset northeast-trending fold and thrust belts.
- one of these faults parallels the Silver Salmon River and another extends along Dry Lake Creek. Silver Salmon fault is the best defined. Motion on these faults may have isolated a deeply exhumed part of the NE-trending thrust belt north of Chikoida Mtn. However, there are no relicts of ultramafite or magnetic response on the east side of the fault that parallels Dry Lake Creek. In fact, a major chert belt occurs on both sides the fault. In order to portray uncertainty with our interpretation, we show a carbonate and a chert layer crossing the projected fault trace south of lower Dry Lake Creek.
- massive carbonate that comprises much of Mt. Sinawa Eddy are part of a folded thrust sheet. Dissection of the sheet by 'Skull Creek' valley show structural discordance in the footwall (Figure 3). A sheet of breccia, semi-conformable with the thrust sole might be syntectonic, and overridden by the fault panels from which it was derived.
- an elongate, thin belt of carbonate that extends up Horsefeed Creek is interpreted as the synformal keel at the southern exposures of the lowest folded thrust sheet of carbonate underlying Mt. Sinawa Eddy. Coeval Middle Permian fusulinid packstone found at a variety of localities within this unit supports such an interpretation. Persistence of a well-bedded limestone layer structurally above the fusulinid packstone-bearing succession also supports the interpretation of a folded, laterally continuous succession. Ages of fusulinids from the packstone and well-bedded succession are Wordian and Roadian versus Leonardian and Roadian respectively (Table 2). Sedimentary structures in the well-bedded succession are right-way-up. These data collectively argue for a thrust contact between the two units, consistent with a structurally complicated zone mapped on the southwestern face of Mt. Sinawa Eddy, which contains horses between 5 and 10 m thick, and several tens of metres long.
- a steeply-dipping fault that cuts the southwestern flank of Mt. Sinawa Eddy appears to carry an antiform in its hangingwall (Photo 6). Several subsidiary block faults offset strata in the fold hinge. The fault is poorly constrained to the south, but it appears to cut across the antiform trace (Figure 3).
- Nearly continuous canyon exposures along the Nakina River and northern tributaries afford a close look at the

extreme structural complexity that characterizes the northern margin of the carbonate belt. Along the lower stretches of Taysen Creek and a parallel tributary to the northeast, informally called "Tumblepack Creek", are excellent exposures of thick-bedded, white carbonate that is thrust imbricated with dark, thin-bedded carbonate. Along the canyon walls of "Tumblepack Creek", more than 20 southeast-verging fault panels can be mapped or inferred (Photo 14). Most are between 5 and 100 m thick and are parallel with a major high-angle fault along which the Nakina River flows for about 750m either side of Taysen Creek. Along the northwestern border of the thrust imbricated belt is a zone of moderately intense folding with 1-10 metre amplitude folds with hinges oriented vertical.

Mihalynuk *et al.* (2002) recognized similar structural imbrication north of lower Horsefeed Creek and attributed it to formation of the Cache Creek accretionary prism. Structural complexity of this type may affect other parts of the carbonate belt, but poor exposure and lack of contrasting strata make recognition difficult.

- Greater structural and stratigraphic coherence can be demonstrated in parts of the carbonate belt. In places, the carbonate belt appears to comprise a sheet resting on the imbricated rocks and folded by northwest-trending folds. In central 104N/2E, an apparent fold closure with Permian carbonate enveloping imbricated Middle Triassic chert was interpreted from 2001 mapping. Critical re-evaluation of this fold hinge in 2002 confirmed a sheared contact in an antiformal closure (Figure 4). The folded fault contact is interpreted to be part of regional fault that soles the carbonate domain (Figure 3).
- Knockers within the serpentinite mélangé belt are commonly discrete lithologies having sharply defined fault contacts. Some faults are strongly curved while others are



Photo 14. Intensely thrust imbrication of lower 'Tumblepack Creek'. Fold hinges and hangingwall cut-offs are consistent with south-verging thrust motion. Enlargement of white boxed area shows complexity of deformation in thin-bedded black limestone. Adjacent panels of thick-bedded, cream-coloured limestone are less deformed. Black boxed inset to left is a view of the canyon wall farther upstream (northwest) where hangingwall and footwall cut-offs are well displayed.

highly planar. Coherent knockers are, in some instances, kilometres across.

NAHLIN FAULT

Nahlin fault forms a discrete contact between Laberge Group strata and ultramafite. Good exposures of serpentinite mélange and Laberge Group wacke can be mapped to within meters of the trace of the Nahlin Fault. Geometric constraints provided by the outcrop distribution require a nearly vertical fault orientation. A steep fault is also indicated by the extreme vertical gradient magnetic anomaly (Lowe and Anderson, 2002). Laberge Group rocks are intensely faulted up to 400m from the Nahlin fault. Structural coherence between northwest-trending fold hinges and bedding cut-offs within the intensely faulted Laberge Group rocks near the fault suggest that most of the faults are southwest-verging thrusts. Some of those nearest the Nahlin fault overturned. Structural intercalation of wacke and serpentinite is conspicuously absent.

Carbonate alteration along the fault produces an intense orange weathering in both Laberge Group rocks and ultramafic rocks adjacent to the fault. Quartz-carbonate-chrome mica alteration of ultramafite (listwanite) is intensely developed in two dilational zones at deflections in the fault trace (Figure 3, localities X, Y): south of lower Goldbottom Creek and both sides of lower Nahlin River.

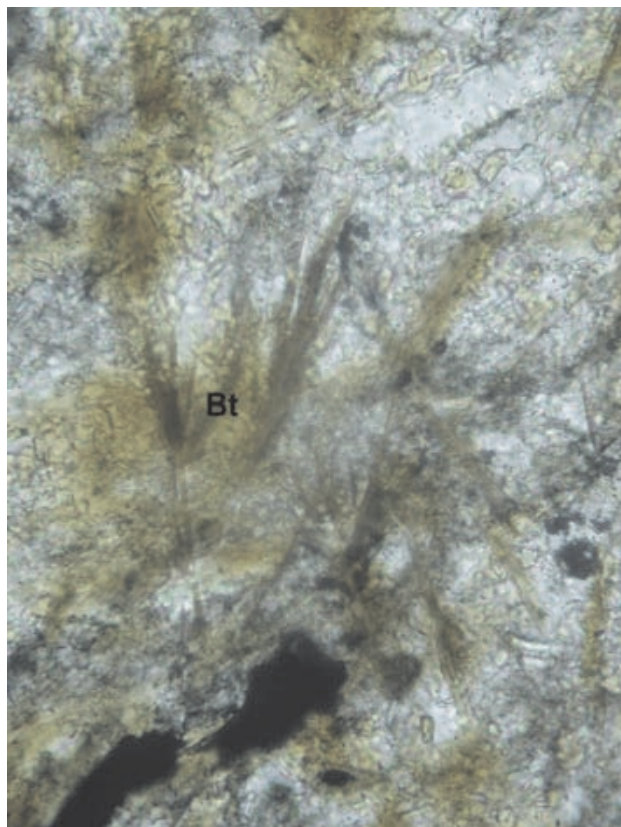


Photo 15. Acicular secondary biotite growth in siliceous argillite 3 km northeast of the Thunder Alley exhalite. Length of photo represents about 4 mm.

Within the Goldbottom zone are quartz-flooded breccia zones up to several metres thick and tens of metres long. Within these zones are small outcrops of only a few square metres of flow-banded rhyolite breccia that we correlate with the Early Eocene Sloko Group. It appears that motion on the fault caused dilation at deflections in the fault trace, permitting intrusion and extrusion of Sloko magmatic rocks and hydrothermal alteration of the adjacent ultramafite. About 50 km to the northwest, the Nahlin fault is plugged by the Birch Mountain pluton. Hornblende from the pluton has been dated by the K/Ar method as 46.3 ± 2.2 Ma (biotite age is slightly older; Bultman, 1979). A sample of the Birch Mountain pluton was collected for U/Pb age dating to test the existing K-Ar age date. Chrome mica from the listwanite was collected for $^{40}\text{Ar}/^{39}\text{Ar}$ age dating to help constrain the age of alteration. Current age data and geological relationships indicate final motion on the fault between ~ 55 and ~ 46 Ma.

MINERAL POTENTIAL

A principal objective of the Nakina transect mapping is mineral resource evaluation. Mineralization and mineralizing environments indicating a variety of prospective deposit types have been observed. In particular, the potential for volcanogenic massive sulphide mineralization is indicated by our 2001 discovery of a magnetite exhalite unit (Thunder Alley occurrence) as well as submarine felsic volcanic rocks underlying parts of drainages with elevated RGS metal values (Mihalynuk *et al.*, 2002). In 2002, quartz-sericite-pyrite schist was discovered up “Tumblepack Creek” and massive sulphide mineralization was discovered north of Hardluck Peaks (named the Joss’alun occurrence; Mihalynuk, 2002; Mihalynuk *et al.*, 2003, this volume). In addition, 0.2 m thick pyrrhotite boulders found near Paradise Peak, are probably related to skarn mineralization. Industrial mineral showings of possible significance include talc lenses east of Chikoida Mountain and long fibre sepiolite from southwest of Mt. O’Keefe. We report on new observations made during the 2002 field season, including additional observations from around the Thunder Alley occurrence. New fossil data from the submarine felsic tuff section is presented above.

MAGNETITE EXHALITE

In 2002, additional field mapping of the regional geological setting of the Thunder Alley magnetite exhalite focused on a search for further mineralization or alteration zones, and collection of stream sediments from drainages surrounding the occurrence. Mineralization at the Thunder Alley exhalite consists of black wispy-laminated magnetite in fine-grained tuffite. Magnetite comprises up to 50% of true thicknesses in excess of 5 metres. Analysis of a 5.3 metre chip sample yielded 16% Fe and 900-1200 ppm Ba. Similar bands occur across a width of 25 metres and can be traced for more than 700 metres (Mihalynuk *et al.*, 2002).

One area, 3 km northeast of Thunder Alley displays evidence of thermal alteration with development of biotite within partings in argillite and ribbon chert. Limits of the

biotite zone were not mapped out in detail, but it is estimated as less than 1 km across. Biotite is not deformed (Photo 15); therefore, it may have formed subsequent to latest regional deformation in the Middle Jurassic. The thermal alteration zone is coincident with the southern margin of a weak positive magnetic anomaly on the aeromagnetic survey map (Dumont *et al.* 2001b). It is noteworthy that the Thunder Alley occurrence is not imaged on the aeromagnetic survey, indicating that substantial accumulations of magnetite are unlikely to be present in the subsurface. Analysis of stream sediments (Table 6) did not reveal metal values in concentrations significantly above background values reported by Jackaman (2000) as part of the regional geochemical survey; however, sampling focused on drainages north of the occurrence.

QUARTZ-SERICITE-PYRITE MINERALIZATION

A rust-weathering zone of intermittently developed quartz-sericite-pyrite mineralization crops out along ~200m of the upper canyon section of `Tumblepack Creek` (Photo 16; location Z on Figure 3). Pyrite comprises up to 15% of the most altered outcrops (MMI02-32-7); although, geochemical analysis of the alteration zone did not reveal base metal concentrations of economic interest.

The cause of this mineralization is not known; however, it occurs on the margin of a positive magnetic anomaly, near the terminus of an eastward-extending salient (Figure 7). The cause of the magnetic anomaly is assumed to be related to an unexposed intrusion. Outcrops closest to the heart of the anomaly are hornfelsed chert cut by a single 2m thick, light pink, feldspar-porphyrific dike.

PARADISE PEAK PYRRHOTITE

Boulders of massive pyrrhotite occur on the south-east flank of the group of steep ridges comprising Paradise



Photo 16. A view up Tumblepack Creek of quartz-sericite-pyrite altered zone.

Peak (Figure 3). Boulders range in size up to 30 by 20 by 15 cm within a talus fan (Photo 17). Part of the talus debris is derived from the thermally metamorphosed contact between Sloko diorite and well-bedded calcareous wacke and argillite of the Laberge Group. Geochemical analysis of the boulder did not return base or precious metal values of interest.

CHIKOIDA MOUNTAIN TALC

Tabular bodies of orange-weathering talc occur near the contact between ultramafic rocks and chert on east flank of Chikoida Mountain. These bodies parallel the fabric within the serpentinite. They are exposed for several metres along strike and are up to a metre or more thick. Talc purity has not been established.

TABLE 5
U-PB ISOTOPIC AGE DATA DETERMINED BY THERMAL IONISATION MASS SPECTROMETRY
AT THE GSC-OTTAWA GEOCHRONOLOGY LABORATORY

F ^a	Wt. ^b mg	U ppm	Pb ^c ppm	²⁰⁶ Pb/ ²⁰⁴ Pb ^d	Pb ^e pg	²⁰⁸ Pb/ ²⁰⁶ Pb ^f	Radiogenic ratios (±1s, %) ^f			Age (Ma, ±2s)		
							²⁰⁷ Pb/ ²³⁵ U	²⁰⁶ Pb/ ²³⁸ U	²⁰⁷ Pb/ ²⁰⁶ Pb	²⁰⁷ Pb/ ²³⁵ U	²⁰⁶ Pb/ ²³⁸ U	²⁰⁷ Pb/ ²⁰⁶ Pb
VN-01-A04 (Z7063; 59.0116°N 132.2279°E)												
Z1 (Z)	367	96	4	22139	0	0.080	0.293±0.15	0.0413±0.14	0.05149±0.07	261.1±0.7	260.9±0.7	263±3
Z2 (Z)	915	91	4	50178	1	0.110	0.294±0.18	0.0414±0.17	0.05152±0.04	261.7±0.8	261.5±0.9	264±2
Z3 (Z)	432	98	4	44523	2	0.110	0.294±0.17	0.0414±0.15	0.05151±0.04	261.7±0.8	261.5±0.8	264±2
Z4 (Z)	283	120	5	36732	2	0.110	0.294±0.15	0.0414±0.13	0.05155±0.06	262.0±0.7	261.6±0.7	266±3
Z5 (Z)	173	222	9	29093	3	0.110	0.294±0.14	0.0414±0.14	0.05154±0.08	261.8±0.7	261.4±0.7	265±4

^aFraction all zircon fractions are abraded; (Z)=Zircon

^bError on weight = ±0.001 mg

^cRadiogenic Pb

^dMeasured ratio corrected for spike and Pb fractionation of 0.09±0.03%/AMU

^eTotal common Pb on analysis corrected for fractionation and spike, of blank model Pb composition

^fCorrected for blank and spike Pb and U and common Pb (Stacey-Kramers model Pb equal to the ²⁰⁶Pb/²³⁸U age)

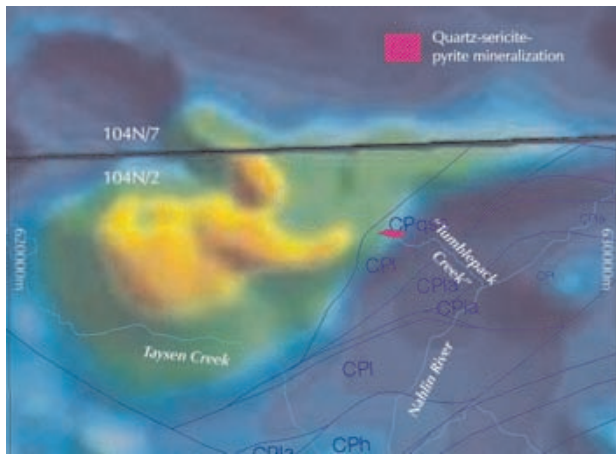


Figure 7. Strong positive magnetic anomaly in north-central 104N/2. Near the eastern limit of the anomaly is the alteration zone on “Tumblepack Creek”.

GREMLIN’S CASTLE SEPIOLITE

Sepiolite occurs along a spiked ridge informally named ‘the Gremlin’s Castle’ 5.6 km south of Mount O’Keefe. Mineralogical identification was made via X-ray diffraction at Teck Cominco Laboratories, Vancouver.

Sepiolite is a hydrated magnesium silicate: $Mg_2Si_3O_8 \cdot 2H_2O$. It has a hollow, tube-like molecular structure, producing a lightweight molecular sieve. Industrial applications are numerous: environmental absorbents, paint thickeners, deodorizers, livestock feed supplements, carriers for fertilizers and pesticides, rubber strengtheners, among others. Sepiolite normally occurs as compact earthy masses, rarely in crystalline form with fibres up to 2cm in length. In this regard, the Gremlin’s Castle sepiolite is unusual. Parallel fibres nearly 20 cm long comprise veins that occur as gashes within quartz-carbonate-chromian mica-altered ultramafite (listwanite). The veins are light grey-green and look like splintered and weathered wood (Photo 18). Sepiolite veins comprise up to ~3% of the out-



Photo 17. Talus block of massive pyrrhotite southeast of Paradise Peak.



Photo 18. Sepiolite vein within listwanite.

crops in which they were observed; however, no accurate assessment of either the extent or abundance of sepiolite veining was made in the field. Because of its unusually fine state of crystallization, the Gremlin’s Castle sepiolite may be useful in specialized applications, or as museum specimens.

SUMMARY AND FUTURE WORK

Geological field studies under the aegis of the Targeted Geoscience Initiative have shown that the Nakina transect area contains geological environments that are prospective for a variety of deposit types. This work has also begun to unravel the structural complexities of the Cache Creek complex and it has forever changed the way that we view its paleotectonic origins.

Of key importance has been the discovery of submarine felsic volcanic rocks of Late Permian to Middle Triassic age; coeval with those hosting volcanogenic massive sulphide accumulations at Kutcho Creek. Volcanic quartz in detrital sediments from a variety of places across the map area points to widespread felsic volcanism within or on the margins of the ancient Cache Creek ocean basin. Indeed, most of the volcanic rocks within the northern Cache Creek terrane are now known to have an intra-oceanic arc affinity. The possibility that Cache Creek felsic or mafic volcanic successions might be associated with mineralised exhalites is demonstrated by vigorous fossil hydrothermal system

TABLE 6
ANALYTICAL RESULTS FROM STREAM SEDIMENTS

Station Number	NAD 83 UTM East	Zone 8 UTM North	Mo ppm	Cu ppm	Pb ppm	Zn ppm	Ag ppb	Ni ppm	Co ppm	Min ppm	Fe %	As ppm	U ppm	Au ppb	Th ppm	Sr ppm	Cd ppm	Sb ppm	Bi ppm	V ppm
FDE02-02-06*	620718	6543146	1.12	77.45	3.28	88.7	74	482.0	44.2	794	4.34	2.8	0.9	1.7	0.9	37.5	0.26	0.22	0.06	88
FDE02-02-07*	620326	6543305	4.26	90.39	5.66	162.0	261	357.2	30.2	1146	3.91	5.2	1.7	3.8	2.0	59.2	0.86	0.70	0.17	102
FDE02-02-10*	620337	6543720	1.39	72.86	3.43	93.9	98	95.7	34.4	991	4.11	3.3	0.3	1.8	0.8	54.5	0.26	0.43	0.06	80
JEN02-34-01	634831	6561399	4.58	69.04	6.88	88.7	100	50.1	17.3	1044	2.97	29.1	1.0	8.9	2.4	30.6	0.63	2.11	0.13	54
JEN02-34-03	632197	6563484	1.84	63.50	4.04	111.0	378	51.3	9.8	995	1.46	6.9	2.2	2.6	0.4	50.7	1.91	0.93	0.08	33
JEN02-34-07	632882	6563228	2.43	60.98	5.52	98.3	89	62.8	16.8	977	2.82	6.1	1.0	3.6	2.2	35.4	0.89	0.68	0.11	57
JEN02-34-09	631915	6563659	0.90	31.45	2.65	102.4	151	31.8	5.3	355	0.92	3.0	1.0	1.2	0.3	76.6	1.88	0.59	0.06	21
MM102-31-05	636985	6568772	0.96	43.82	5.13	145.3	79	76.2	17.8	899	2.88	6.5	0.6	3.8	1.5	32.3	1.77	0.48	0.09	60
MM102-31-13	636792	6567445	1.54	39.40	4.90	128.3	52	77.7	18.0	2004	2.84	5.3	0.7	3.1	1.3	28.0	1.00	0.39	0.10	58
MM102-31-14	636434	6566341	1.56	72.10	8.48	190.3	90	60.6	14.8	1364	2.58	6.3	1.7	1.8	1.2	28.9	2.64	0.77	0.15	39
MM102-31-15	636106	6566229	1.00	45.70	5.81	155.5	44	82.3	16.8	884	3.10	5.1	0.5	2.1	1.1	32.4	1.40	0.48	0.10	69
MM102-32-07 ^{sc}	626552	6568582	44.90	70.65	25.49	95.2	466	29.7	7.9	330	7.60	35.2	2.8	<.2	8.3	144.6	0.58	0.87	2.83	47
MM102-32-11	625919	6568900	1.29	6.14	1.36	25.0	20	9.4	3.0	229	0.80	0.9	1.4	0.6	1.4	21.1	0.09	0.09	0.02	23
MM102-34-05*	620872	6544094	2.85	57.15	4.09	126.0	56	67.9	24.5	1006	4.32	5.5	0.4	0.9	0.4	65.5	0.50	0.46	0.06	106
MM102-35-10	602970	6565290	0.64	24.11	2.60	59.7	37	330.8	29.8	1019	3.11	3.0	0.3	0.9	1.2	21.7	0.14	0.20	0.05	61
ORO02-28-08	636207	6568194	0.98	47.83	5.50	92.7	104	77.2	16.6	498	2.88	15.9	0.6	18.1	1.9	29.3	0.56	0.89	0.11	67
ORO02-30-02	620501	6568418	0.42	3.66	1.54	18.5	19	5.6	2.1	184	0.77	0.6	0.7	0.2	0.6	17.0	0.11	0.08	<.02	22
Red Dog Standard			13.93	163.65	7.42	54.1	84	12.6	11.7	438	4.18	6.0	0.4	22.0	1.1	48.9	0.22	0.21	0.55	99

Station Number	Ca %	P %	La ppm	Cr ppm	Mg %	Ba ppm	Ti %	B ppm	Al %	Na %	K %	W ppm	Sc ppm	Tl ppm	S %	Hg ppb	Se ppm	Te ppm	Ga ppm
FDE02-02-06*	1.10	0.046	5.0	395.0	5.49	114.2	0.130	11	2.17	0.016	0.07	<.1	9.0	0.06	0.04	41	0.9	0.03	6.6
FDE02-02-07*	0.81	0.075	9.0	215.1	3.51	689.5	0.133	2	2.08	0.022	0.22	<.1	7.9	0.24	0.08	67	2.1	0.08	7.6
FDE02-02-10*	1.14	0.063	6.6	88.3	1.72	167.3	0.053	5	1.69	0.015	0.13	<.1	10.3	0.11	0.09	47	0.6	0.05	5.4
JEN02-34-01	0.89	0.071	11.6	38.9	0.79	170.1	0.105	1	1.10	0.006	0.08	<.1	4.4	0.11	0.04	105	0.8	0.08	4.0
JEN02-34-03	4.88	0.124	9.3	110.3	1.45	204.3	0.038	8	0.75	0.010	0.09	<.1	1.9	0.26	0.18	150	5.5	0.03	3.0
JEN02-34-07	1.31	0.119	14.2	65.6	1.33	115.6	0.126	1	1.36	0.006	0.11	<.1	4.1	0.10	0.03	66	0.9	0.05	4.9
JEN02-34-09	16.75	0.077	7.0	41.7	1.38	133.8	0.026	3	0.41	0.006	0.05	<.1	1.4	0.12	0.08	63	1.6	0.03	1.6
MM102-31-05	1.21	0.115	13.4	104.8	1.57	201.0	0.114	2	1.53	0.007	0.13	<.1	4.7	0.09	0.07	83	1.7	0.02	5.5
MM102-31-13	0.99	0.088	10.7	94.6	1.45	277.3	0.105	1	1.41	0.008	0.13	<.1	4.0	0.10	0.06	39	2.4	0.05	5.3
MM102-31-14	1.18	0.228	21.1	41.6	1.03	231.3	0.041	2	1.45	0.004	0.15	<.1	3.7	0.20	0.05	99	0.4	0.06	5.0
MM102-31-15	1.03	0.133	15.0	91.2	1.70	175.8	0.105	3	1.75	0.006	0.17	<.1	4.9	0.10	0.06	42	0.8	0.05	6.2
MM102-32-07 ^{sc}	0.11	0.171	18.3	19.9	0.72	125.3	0.139	1	0.82	0.143	0.62	8	2.3	0.58	1.64	23	15.9	0.24	4.0
MM102-32-11	0.41	0.095	8.2	17.7	0.27	182.7	0.044	<.1	0.70	0.018	0.05	<.1	1.3	0.05	0.02	8	0.3	<.02	2.4
MM102-34-05*	0.81	0.041	3.7	69.9	2.19	36.0	0.157	4	2.35	0.026	0.05	<.1	9.7	0.19	0.04	35	0.6	0.03	7.8
MM102-35-10	0.67	0.060	7.5	367.9	3.74	93.0	0.107	4	1.34	0.007	0.04	<.1	5.4	0.05	0.02	171	0.3	0.02	4.6
ORO02-28-08	1.00	0.117	13.3	110.6	1.68	183.6	0.113	3	1.56	0.010	0.15	<.1	6.3	0.12	0.04	120	0.9	0.03	5.3
ORO02-30-02	0.40	0.069	5.0	14.4	0.17	87.0	0.035	<.1	0.41	0.018	0.03	<.1	0.7	0.03	0.02	7	0.4	<.02	1.3
Red Dog Standard	0.68	0.057	4.6	22.5	0.69	53.6	0.138	<.1	1.84	0.021	0.03	0.1	4.8	0.03	0.65	17	3.2	0.41	6.0

Analyses by ACME Analytical Laboratories, Vancouver

Sediment sample sieved to -80 mesh @ ACME.

Aqua regia digestion; ICPMS (1 gram sample)

* as station number suffix indicates a sample collected in the drainage underlying the Joss-alun discovery

^{sc} as station number suffix indicates a soil composite (mainly fine talus)

that comprises the Thunder Alley occurrence. Thermal metamorphism of Cache Creek strata northeast of Thunder Alley may be related to the hydrothermal system responsible for the exhalite. Our follow-up mapping and stream sediment sampling around Thunder Alley focused on the area north of the occurrence. More prospecting and geochemical evaluation of the area is required to properly assess the potential for mineralization in the area.

The origin of massive copper sulphide at the new Joss'alun discovery is uncertain, but sulphide lenses appear to be at least partly concordant, and possibly syngenetic with submarine volcanic rocks (more discussion in the following paper).

Structural and stratigraphic advances in our understanding of the Nakina transect have benefited from the rapid expansion of paleontological and isotopic age data. Production of 1:50 000 scale maps will be aided by ~140 new radiolarian collections; ~65 new collections of Carboniferous to Permian fusulinids; 9 Carboniferous, Permian and Triassic conodont collections, and numerous macrofossil collections including Permian ammonoids and Carboniferous corals. New structural, stratigraphic and age data, in combination with petrochemical studies (*e.g.* English *et al.*, 2002), permit us to suggest the following tectonic history:

- Late Permian rupture of oceanic crust and formation of the intra-oceanic Kutcho arc, perhaps more than 2500 km long. Submarine massive sulphide mineralization accumulates within the arc setting. A lack of rocks older than Early Carboniferous suggests that the rupture occurred across oceanic crust of this age and younger.
- Strata incorporated into the forearc and accretionary complex retain an oceanic signature until Middle or Late Triassic time when quartz-rich detritus is derived from exhumation of the Kutcho arc.
- By Early Jurassic time, detritus carries Devonian-Mississippian zircons signalling influx from Stikine, Quesnel and/or Yukon-Tanana terranes (may all be broadly considered parts of the same arc complex; *e.g.* Mihalynuk *et al.*, 1994). The northern Quesnel arc segment amalgamated with an ancestral continental margin assemblage at 186 Ma (Nixon *et al.*, 1993).
- In Early Middle Jurassic time (~173 Ma Mihalynuk *et al.*, 1999) the Stikine arc segment and intervening Cache Creek complex collided with the Quesnel arc segment. Because the Quesnel arc was already welded to an inboard continental domain (North America or an outboard ribbon continent; *e.g.* Johnston, 2001), it acted as a rigid backstop, and drove the intervening Cache Creek accretionary complex southwest over the forearc Laberge Group strata of the Stikine arc segment. Southwest-verging fold and thrust belt deformation in the previously undeformed Laberge Group records the collision. Superposition of this deformational episode on thrust faulted accretionary complex resulted in (re)folding, reactivation, and/or reimbrication by younger thrust faults.
- Emplacement-related structures in Cache Creek terrane are extensively cut by Middle Jurassic plutons ~172Ma. Hydrothermal alteration of ultramafite adjacent to the

Chikoida stock may have facilitated formation of tabular bodies of talc.

- Dextral motion on the Nahlin fault occurred, at least intermittently, until Eocene time. Motion around 55 Ma may have facilitated crustal transit of Sloko Group magma and eruption of continental arc volcanic rocks and comagmatic plutons. Extensive zones of listwanite at deflections in the fault trace may record hydrothermal fields related to Sloko magmatism. Post Sloko dilation resulted in gash veins infilled with sepiolite.
- By ~46 Ma the Nahlin fault is plugged by the Birch Mountain pluton.

ACKNOWLEDGEMENTS

Success of the Nakina transect mapping program is due to the combined effort of a dedicated mapping team who made full use of the midnight sun (or lack thereof). Those not acknowledged through co-authorship are: Adam Bath, Jacqueline Blackwell, Oliver Roenitz, Lucinda Leonard and Fionnuala Devine; all delivered a rock-solid effort. Sincere thanks to the Atlin TGI leader, Carmel Lowe of the Pacific Geoscience Centre (GSC), who took care of endless paperwork in order to secure the TGI funding for mapping in 2002. Jim Monger thoughtfully offered us the use of his unpublished field maps. Numerous individuals aided in geological mapping or contributed to our work through stimulating discussions (at times slurred) at our base camp in Atlin.

For a second consecutive field season, Norm Graham of Discovery Helicopters in Atlin extended service beyond the limits of our budget, and beyond the limits of reasonable flying conditions. Rita Scott and Nora (Kuya) Minogue shared with us their home and folklore. Thanks also to the many other people of Atlin who offer their continued enthusiastic support of our field programs.

REFERENCES CITED

- Aitken, J.D. (1959): Atlin map-area, British Columbia; *Geological Survey of Canada*, Memoir 307, 89 pages.
- Ash, C.H. (1994): Origin and tectonic setting of ophiolitic ultramafic and related rocks in the Atlin area, British Columbia (NTS 104N); *B.C. Ministry of Energy, Mines and Petroleum Resources*, Bulletin 94, 48 pages.
- Bath, A. (2003): Atlin TGI, Part IV: Middle Jurassic granitic plutons within the CacheCreek terrane and their aureoles: Implications for terrane emplacement and deformation; in *Geological Fieldwork 2002*, *BC Ministry of Energy and Mines*, Paper 2003-1, this volume.
- BCMÉM (1978): Atlin Regional Geochemical Survey, 882 sites plus 160 lake sites; *BC Ministry of Energy and Mines and the Geological Survey of Canada*, RGS 51.
- Bilsland, W.W. (1952): Atlin, 1898-1910: The story of a gold boom; *British Columbia Historical Quarterly*, Volume 16, Numbers 3 and 4 (Reprinted in 1971 by the Atlin Centennial Committee, 63 pages with pictorial supplement).
- Bloodgood, M.A. and Bellefontaine, K.A. (1990): The geology of the Atlin area (Dixie Lake and Teresa Island) (104N/ 6 and parts of 104N/ 5 and 12); in *Geological Fieldwork*, 1989, *B.C. Ministry of Energy, Mines and Petroleum Resources*, Paper 1990-1, pages 205-215.

- Childe, F.C. and Thompson, J.F.H. (1997): Geological setting, U-Pb geochronology, and radiogenic isotopic characteristics of the Permo-Triassic Kutcho Assemblage, north-central British Columbia; *Canadian Journal of Earth Sciences*, Volume 34, pages 1310-1324.
- Childe, F.C., Thompson, J.F.H., Mortensen, J.K., Friedman, R.M., Schiarizza, P., Bellefontaine, K. and Marr, J.M. (1998): Primitive Permo-Triassic volcanism in the Canadian Cordillera tectonic and metallogenic implications; *Economic Geology and the Bulletin of the Society of Economic Geologists*, Volume 93, pages 224-231.
- Coney, P.J., Jones, D.L. and Monger, J.W.H. (1980): Cordilleran suspect terranes; *Nature (London)*, Volume 288, pages 329-333.
- Cordey, F., Gordey, S.P., Orchard, M.J. and Canada, G.S. (1991): New biostratigraphic data for the northern Cache Creek Terrane, Teslin map area, southern Yukon; in Current research; Part E—Recherches en cours; Partie E., *Geological Survey of Canada*, pages 67-76.
- Devine, F.A.M. (2002): U-Pb geochronology, geochemistry, and tectonic implications of oceanic rocks in the northern Cache Creek terrane, Nakina area, northwestern British Columbia; *The University of British Columbia*, Vancouver, unpublished B.Sc. thesis, 50 pages.
- Dumont, R., Coyle, M. and Potvin, J. (2001a): Aeromagnetic total field map British Columbia: Nakina Lake, NTS 104N/1; *Geological Survey of Canada*, Open File, 4091.
- Dumont, R., Coyle, M. and Potvin, J. (2001b): Aeromagnetic total field map British Columbia: Nakina, NTS 104N/2; *Geological Survey of Canada*, Open File, 4092.
- Dumont, R., Coyle, M. and Potvin, J. (2001): Aeromagnetic total field map British Columbia: Sloko River, NTS 104N/3; *Geological Survey of Canada*, Open File, 4093.
- English, J.M., Mihalynuk, M.G., Johnston, S.T. and Devine, F.A. (2002): Atlin TGI Part III: Geology and Petrochemistry of mafic rocks within the northern Cache Creek terrane and tectonic implications; in Geological Fieldwork 2001, *B.C. Ministry of Energy and Mines*, Paper 2002-1, pages 19-29.
- English, J.M., Mihalynuk, M.G., Johnston, S.T., Orchard, M.J., Fowler, M. and Leonard, L.J. (2003): Atlin TGI, Part VI: Early to Middle Jurassic sedimentation, deformation and a preliminary assessment of hydrocarbon potential, central Whitehorse Trough and northern Cache Creek terrane; in Geological Fieldwork 2002, *BC Ministry of Energy and Mines*, Paper 2003-1, this volume
- Gordey, S.P., McNicoll, V.J. and Mortensen, J.K. (1998): New U-Pb ages from the Teslin area, southern Yukon, and their bearing on terrane evolution in the northern Cordillera; in Radiogenic age and isotopic studies; Report 11., *Geological Survey of Canada*, pages 129-148.
- Harker, P. (1953): Report on fossil collections submitted by R.L. Christie and J.D. Aitken from the Bennett Lake and Atlin Lake area; *Geological Survey of Canada*, unpublished Fossil Report, P7, 2 pages.
- Hart, C.J.R., Dickie, J.R., Ghosh, D.K. and Armstrong, R.L. (1995): Provenance constraints for Whitehorse Trough conglomerate; U-Pb zircon dates and initial Sr ratios of granitic clasts in Jurassic Laberge Group, Yukon Territory; in Jurassic magmatism and tectonics of the North American Cordillera., Miller, David, M ; Busby and Cathy (Editors), *Geological Society of America*, Special Paper 299, pages 47-63.
- Jackaman, W. (2000): British Columbia Regional Geochemical Survey, NTS 104N/1 - Atlin; *BC Ministry of Energy and Mines*, BC RGS, 51.
- Johnston, S.T. (2001): The Great Alaskan Terrane Wreck: reconciliation of paleomagnetic and geological data in the northern Cordillera; *Earth and Planetary Science Letters*, Volume 193, pages 259-272.
- Krough, T.E. (1982): Improved accuracy of U-Pb ages by the creation of more concordant systems using an air abrasion technique; *Geochimica et Cosmochimica Acta*, Volume 46, pages 637-649.
- Lefebure, D. V. and Gunning, M. H. (1988): Gold litho-geochemistry of Bronson Creek area, British Columbia; in Exploration in British Columbia; 1987., Anonymous (Editor), *British Columbia Ministry of Mines and Petroleum Resources*, 1987, pages B71-B77.
- Lowe, C. and Anderson, R.G. (2002): Preliminary interpretation of new aeromagnetic data for the Atlin Map area, British Columbia; in Current Research, Part A, *Geological Survey of Canada*, Paper 2002-A17, page 10.
- Lowe, C., Mihalynuk, M.G., Anderson, R.G., Canil, D., Cordey, F., English, J.M., M. H., Johnston, S.T., M. O., Russell, J.K., Sano, H. and Villeneuve, M. (2003): Atlin TGI Project overview, northwestern British Columbia, year three; in Current Research, Part A, *Geological Survey of Canada*, Paper 2003-, this volume.
- Merran, Y. (2002): Mise en place et environnement de depot d'une plate-forme carbonatee intraoceanique: exemple du complexe d'Atlin, Canada; *Université Claude Bernard*, Lyon, France, unpublished M.Sc. thesis, 50 (and appendices) pages.
- Mihalynuk, M.G. and Smith, M.T. (1992): Highlights of 1991 mapping in the Atlin-West Map area (104N/12); in Geological fieldwork 1991; a summary of field activities and current research., Grant and B ; Newell (Editors), *Province of British Columbia, Ministry of Energy, Mines and Petroleum Resources*, pages 221-227.
- Mihalynuk, M.G., Nelson, J. and Diakow, L.J. (1994): Cache Creek Terrane entrapment; oroclinal paradox within the Canadian Cordillera; *Tectonics*, Volume 13, pages 575-595.
- Mihalynuk, M.G., Meldrum, D., Sears, S. and Johannson, G. (1995): Geology and mineralization of the Stuhini Creek area (104K/11); in Geological fieldwork 1994; a summary of field activities and current research., Grant and B ; Newell (Editors), *BC Ministry of Energy, Mines and Petroleum Resources*, pages 321-342.
- Mihalynuk, M.G., Bellefontaine, K.A., Brown, D.A., Logan, J.M., Nelson, J.L., Legun, A.S. and Diakow, L.J. (1996): Geological compilation, northwest British Columbia (NTS 94E, L, M; 104F, G, H, I, J, K, L, M, N, O, P; 114J, O, P); *BC Ministry of Energy and Mines*, Open File, 1996-11.
- Mihalynuk, M.G. and Cordey, F. (1997): Potential for Kutcho Creek volcanogenic massive sulphide mineralization in the northern Cache Creek Terrane; a progress report; in Geological fieldwork 1996; a summary of field activities and current research., Lefebure, V ; McMillan and J ; McArthur (Editors), *BC Ministry of Energy, Mines and Petroleum Resources*, Paper 1997-1, pages 157-170.
- Mihalynuk, M.G., Erdmer, P., Ghent, E.D., Archibald, D.A., Friedman, R.M., Cordey, F., Johannson, G.G. and Beanish, J. (1999): Age constraints for emplacement of the northern Cache Creek Terrane and implications of blueschist metamorphism; *BC Ministry of Energy, Mines and Petroleum Resources*, Paper 1999-1, 127-142 pages.
- Mihalynuk, M.G. (2002): Geological setting and style of mineralization at the Joss'alun discovery, Atlin area, British Columbia; *BC Ministry of Energy and Mines*, Geofile, GF2002-6, 4 (plus digital presentation) pages.
- Mihalynuk, M.G., Johnston, S.T., Lowe, C., Cordey, F., English, J.M., Devine, F.A.M., Larson, K. and Merran, Y. (2002): Atlin TGI Part II: Preliminary results from the Atlin Targeted Geoscience Initiative, Nakina Area, Northwest British Columbia; in Geological Fieldwork 2001, *BC Ministry of Energy and Mines*, Paper 2002-1, pages 5-18.
- Monger, J.W.H. (1969): Stratigraphy and structure of Upper Paleozoic rocks, northeast Dease Lake map-area, British Colum-

- bia (104J); Ottawa, ON, Canada, Geological Survey of Canada, 41 pages.
- Monger, J.W.H. (1975): Upper Paleozoic rocks of the Atlin Terrane, northwestern British Columbia and south-central Yukon; *Geological Survey of Canada*, Paper 74-47, 63 pages.
- Nixon, G.T., Archibald, D.A. and Heaman, L.M. (1993): (^{40}Ar - ^{39}Ar) Ar and U-Pb geochronometry of the Polaris alaskan-type complex, British Columbia; precise timing of Quesnellia-North America interaction; in Geological Association of Canada; Mineralogical Association of Canada; annual meeting; program with abstracts, *Geological Association of Canada*, page 76.
- Okulitch, A.V. (1999): Geological time scale, 1999; *Geological Survey of Canada*, National Earth Science Series, Geological Atlas, Open File 3040, wall chart - revision pages.
- Parrish, R.R., Roddick, J.C., Loveridge, W.D. and Sullivan, R.W. (1987): Uranium-lead analytical techniques at the Geochronology Laboratory, Geological Survey of Canada; in Radiogenic Age and Isotopic Studies: Report 1, *Geological Survey of Canada*, Paper 87-2, pages 3-7.
- Renne, P.R., Deino, A.L., Walter, R.C., Turrin, B.D., Swisher, C.C.I., Becker, T.A., Curtis, G.H., Sharp, W.D. and Jaouni, A.R. (1994): Intercalibration of astronomical and radioisotopic time; *Geology*, Volume 22, pages 783-786.
- Roddick, J.C. (1987): Generalized numerical error analysis with applications to geochronology and thermodynamics; *Geochimica et Cosmochimica Acta*, Volume 51, pages 2129-2135.
- Roddick, J.C. (1988): The assessment of errors in $^{40}\text{Ar}/^{39}\text{Ar}$ dating; in Radiogenic Age and Isotopic Studies, Report 2, *Geological Survey of Canada*, Paper 88-2, pages 7-16.
- Schiarizza, P., Massey, N. and MacIntyre, D.G. (1998): Geology of the Sitlika Assemblage in the Takla Lake area (93N/ 3, 4, 5, 6, 12), central British Columbia; in Geological fieldwork 1997; a summary of field activities and current research., Smyth (Editor), *British Columbia Geological Division*, pages 4.1-4.19.
- Terry, J. (1977): Geology of the Nahlin ultramafic body, Atlin and Tulsequah map-areas, northwestern British Columbia; in Current Research, Part A, *Geological Survey of Canada*, pages 263-266.
- Villeneuve, M.E. and MacIntyre, D.G. (1997): Laser $^{40}\text{Ar}/^{39}\text{Ar}$ ages of the Babine porphyries and Newman Volcanics, Fulton Lake map area, west-central British Columbia; in Radiogenic Age and Isotopic Studies, Report 10, *Geological Survey of Canada*, Current Research 1997-F, pages 131-139.
- Villeneuve, M.E., Sandeman, H.A. and Davis, W.J. (2000): A method for the intercalibration of U-Th-Pb and $^{40}\text{Ar}/^{39}\text{Ar}$ ages in the Phanerozoic; *Geochimica et Cosmochimica Acta*, Volume 64, pages 4017-4030.

